

Synthesis of Unsymmetrical N-Carboranyl NHCs: Directing Effect of the Carborane Anion

Matthew Asay,^b Steven P. Fisher,^a Sarah E. Lee,^a

Fook S. Tham,^a Dan Borchardt^a and Vincent Lavallo*^a

^a Department of Chemistry University of California, Riverside, Riverside, CA 92521 (USA).

vincent.lavallo@ucr.edu

^b Instituto de Química, Universidad Nacional Autónoma de México, Circuito Exterior, Ciudad Universitaria, México, D.F. 04360, (México).

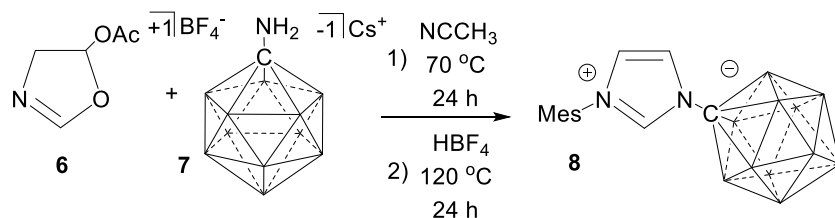
Supporting Information

General considerations	S2
Synthesis and spectra of zwitterionic imidazolium, 8	S3-S9
Synthesis and spectra of monoanionic lithium carbene, Li[9]	S9-S13
Synthesis and spectra of monoanionic potassium carbene, K[9]	S13-S18
Synthesis and spectra of dianionic lithium dicarbene, Li₂[10]	S19-S24
X-Ray Crystal Data of Li[9]	S25-S27
X-Ray crystal Data of Li₂[10]	S28-S30
References	S31

General Considerations:

All manipulations were carried out using standard Schlenk or glovebox techniques under a dinitrogen or argon atmosphere unless otherwise stated. Dry solvents were obtained via distillation under argon from potassium (benzene and toluene), calcium hydride (acetonitrile and methylene chloride), sodium-potassium alloy (diethyl ether), or potassium benzophenone ketyl (THF). Cesium 1-amino-1-carba-*closo*-undecaborate **7** was prepared following the procedure by Jelínek and co-workers.⁽¹⁾ The 1-mesityl-3-acetoxyoxazolinium tetrafluoroborate **6** was prepared via the Fürstner synthetic route.⁽²⁾ Unless specifically stated, reagents were purchased from commercial vendors and used without further purification. Nuclear magnetic resonance (NMR) spectroscopy was carried out using: Bruker Avance 300 MHz, Bruker Avance 600 MHz, Varian Inova 300 MHz, or Varian Inova 400 MHz spectrometers. NMR chemical shifts are reported in parts per million (ppm) with ¹H and ¹³C chemical shifts referenced to the residual non-deutero solvent. The ¹¹B NMR chemical shifts were externally referenced to BF₃•OEt₂. The ¹¹B-¹H coupling constants from ¹¹B spectra are reported when possible. The 2D NOESY data were collected using a modified version of the standard Bruker NOESY sequence 'noesygpph'. Decoupling of ¹¹B in the F1 dimension was achieved by inserting a 180 degree ¹¹B pulse midway through the t1 evolution period. Decoupling of ¹¹B in the F2 dimension was achieved by applying broadband GARP ¹¹B decoupling during the acquisition period. Data sets were collected as 1024 x 256 complex point arrays using States-TPPI phase cycling. Sixteen transients were averaged for each t1 increment. Data processing consisted of linear prediction in F1, application of a 90 degree shifted sine bell apodization function in both F1 and F2, and Fourier Transformation with zero filling resulting in a 1024 x 1024 point real array. Two IR instruments were used, PIKE MB3000 and a PerkinElmer Spectrum One. High-resolution mass spectrometry (HRMS) was collected on an Agilent Technologies 6210 (TOF LC/MS) featuring electrospray ionization. Melting points were acquired using a Büchi Melting Point B-545 automatic. Complete crystallographic data for compounds **Li[9]** and **Li₂[10]** are available free of charge from the Cambridge Crystallographic Data Center under reference numbers 1028440 and 1028443, respectively. These structures can be accessed at : <http://www.ccdc.cam.ac.uk/Community/Requestastructure/Pages/DataRequest.aspx>.

Synthesis of the zwitterionic imidazolium, 8:



A Teflon stoppered Schlenk was equipped with a stir bar and loaded with compound **6** (1.515 g, 4.52 mmol) and cesium 1-amino-1-carba-*closo*-undecaborate **6** (1.45 g, 4.97 mmol). Dry acetonitrile (4 mL) was added to the schlenk which was tightly sealed and heated to 70°C for 24 hours. To the crude reaction mixture tetrafluoroboric acid diethyl ether complex (1.35 mL, 1.61 mmol) was added. The Schlenk was sealed and heated to 110°C for 24 hours (safety note: heating sealed containers is dangerous and was always done in a hood behind a blast shield using a thick-walled Schlenk tube, appropriate precautions should always be taken). The solution was cooled then poured into a beaker containing sodium bicarbonate (200 mL). Methylene chloride (200 mL) was added and the aqueous phase was further washed with methylene chloride (2 × 100 ml). The organic phase was collected, washed with brine (300 ml) and dried over magnesium sulfate. All volatiles were subsequently removed under vacuum to give a brown solid. This solid was crystallized from a concentrated acetonitrile solution at 5°C to give **8** as light colorless blocks. Further concentration of the supernate led to two further crops of crystals (1.14 g, 77%). ¹H NMR (500 MHz, acetonitrile-d₃, 25°C): δ = 8.76 (dd, ⁴*J*(H,H) = 2.0, 1.8 Hz, 1H), 7.73 (dd, ³*J*(H,H) = 2.0 Hz, ⁴*J*(H,H) = 1.8 Hz, 1H), 7.34 (dd, ⁴*J*(H,H) = 2.0 Hz, ³*J*(H,H) = 2.0 Hz, 1H), 7.09 (s, 2H), 2.34 (s, 3H), 1.98 (s, 6H), 2.72-1.22 (bm, 11H, B-H). ¹H[¹¹B] NMR (192.5 MHz, acetonitrile-d₃, 25°C): δ = 8.76 (1H), 7.73 (1H), 7.34 (1H), 7.09 (2H), 2.34 (3H), 1.98 (6H), 2.14 (5H), 1.68 (6H). ¹³C[¹H] NMR (125 MHz, acetone-d₆, 25°C): δ = 142.0, 137.6, 135.3, 132.0, 130.3, 124.8, 124.7, 76.4, 21.0, 17.2 ppm. ¹¹B[¹H] NMR (192.5 MHz, acetonitrile-d₃, 25°C): δ = -8.3, -12.7, -13.3 ppm. ¹¹B[¹H] NMR (96 MHz, acetonitrile-d₃, 25°C) = -9.2, -13.5 ppm. ¹¹B NMR (96 MHz, THF-d₈, 25°C): δ = -8.7 (¹*J*(H,B) = 134.4 Hz), -13.4 (¹*J*(H,B) = 137.3 Hz). IR (solid, ATR, 25°C): B-H stretch = 2550 cm⁻¹. HRMS (negative mode ESI/APCI) [M-H]⁻ m/z Calc: C₁₃H₂₄10B₂11B₉N₂ = 327.3041: Found = 327.3041. m.p. = 286.8 to 287.7°C.

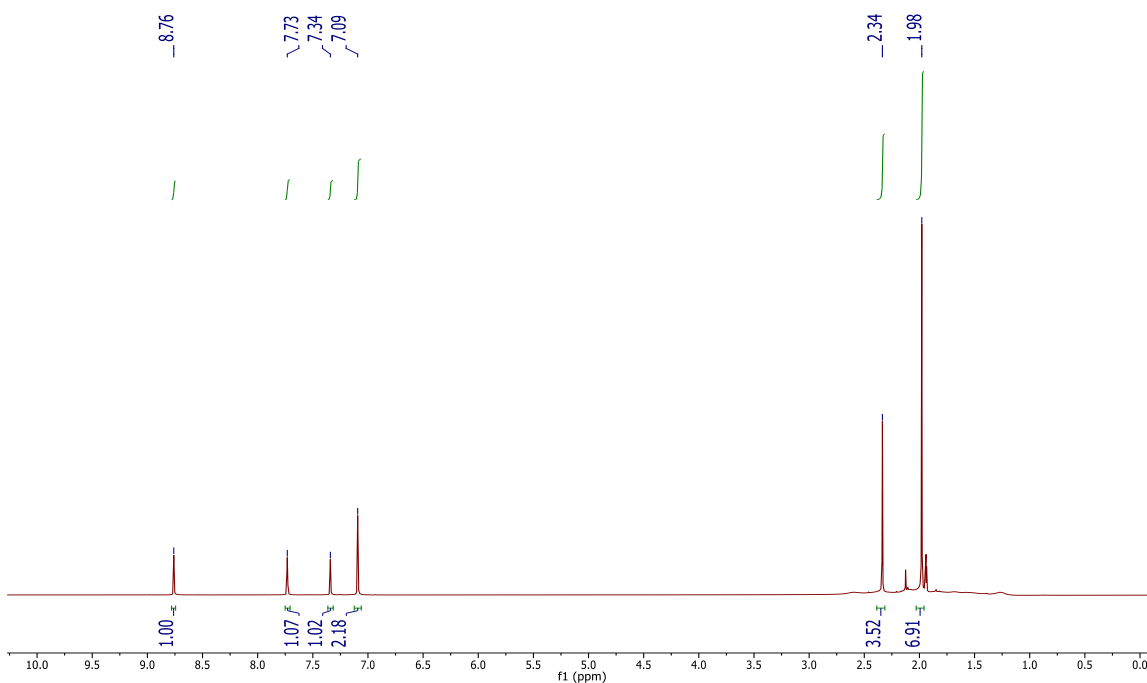


Fig. S1. $^1\text{H-NMR}$ spectrum of **8** in acetonitrile- d_3 . The peak at 2.2 ppm is due to water in the deuterated solvent.

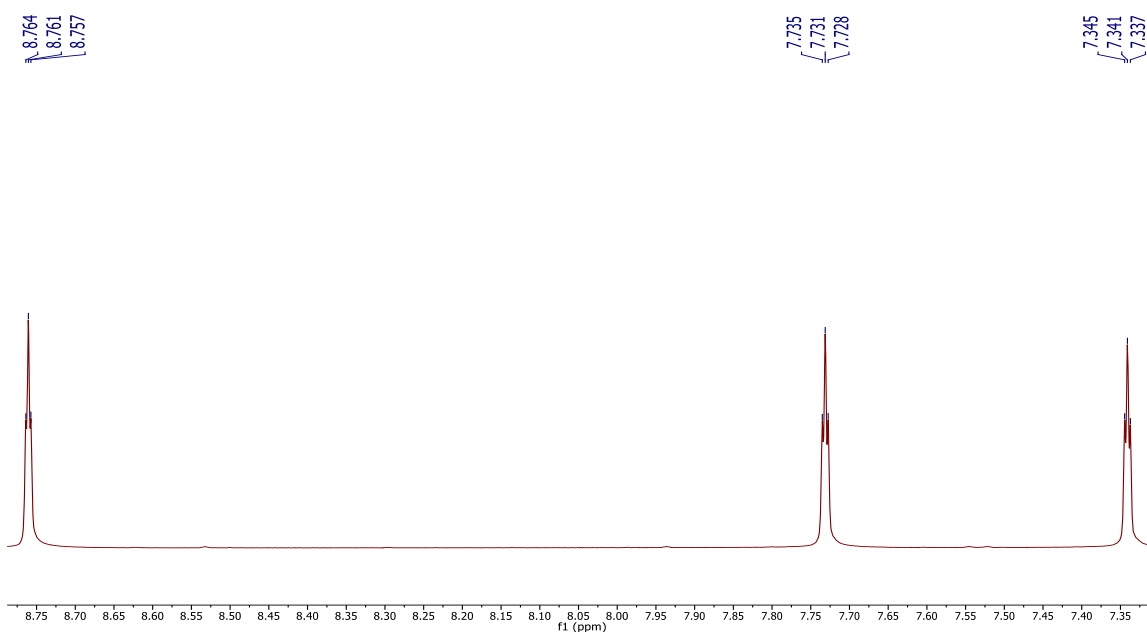


Fig. S2. An expanded view of the aromatic region of the $^1\text{H-NMR}$ of **8** in THF-d_8 , showing the small J -coupling of the imidazolium protons.

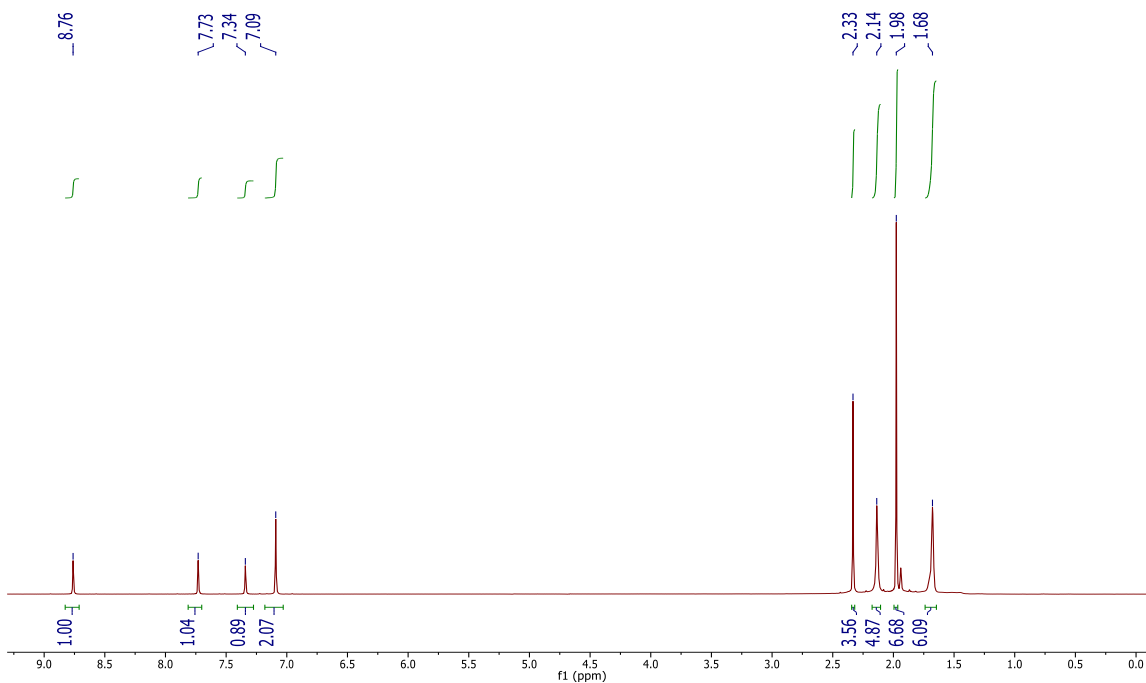


Fig. S3. $^1\text{H}[^{11}\text{B}]$ NMR spectrum of **8** in acetonitrile- d_3 . The boron hydrides appear at 2.14 and 1.68 ppm.

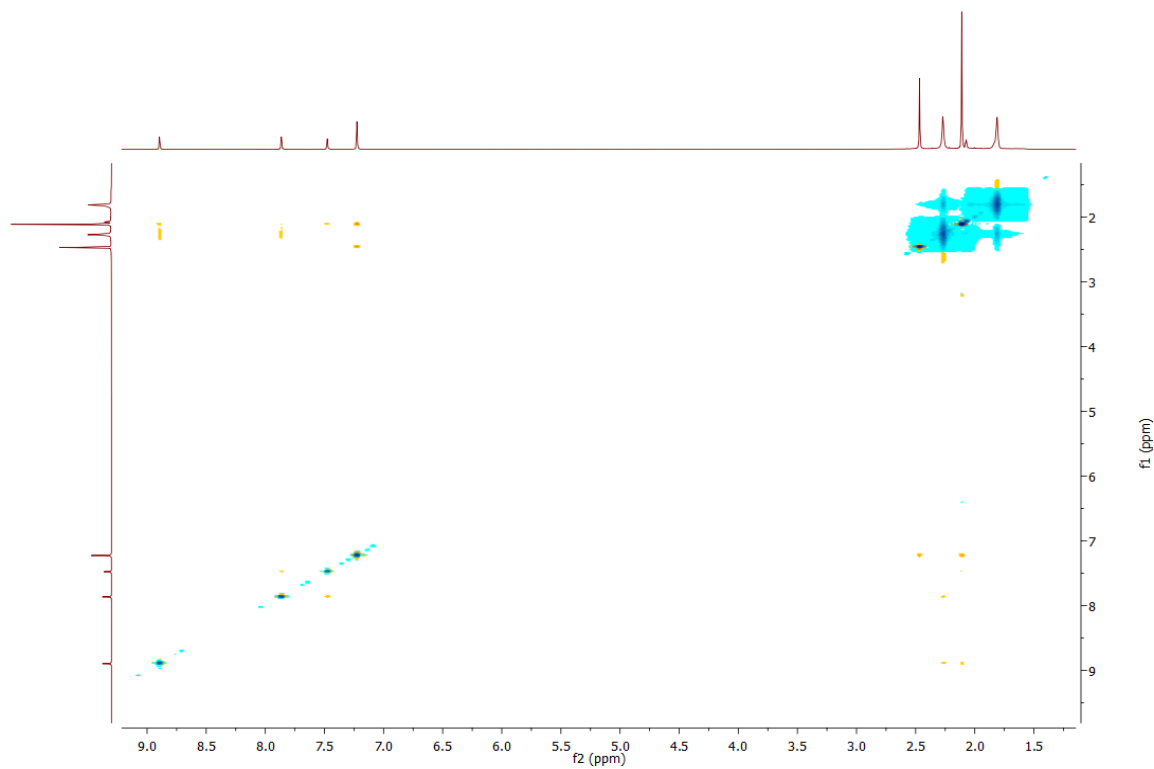


Fig. S4. $^1\text{H}[^{11}\text{B}]$ -NOESY NMR spectrum of **8** in acetonitrile- d_3 , mixing time = 500 ms.

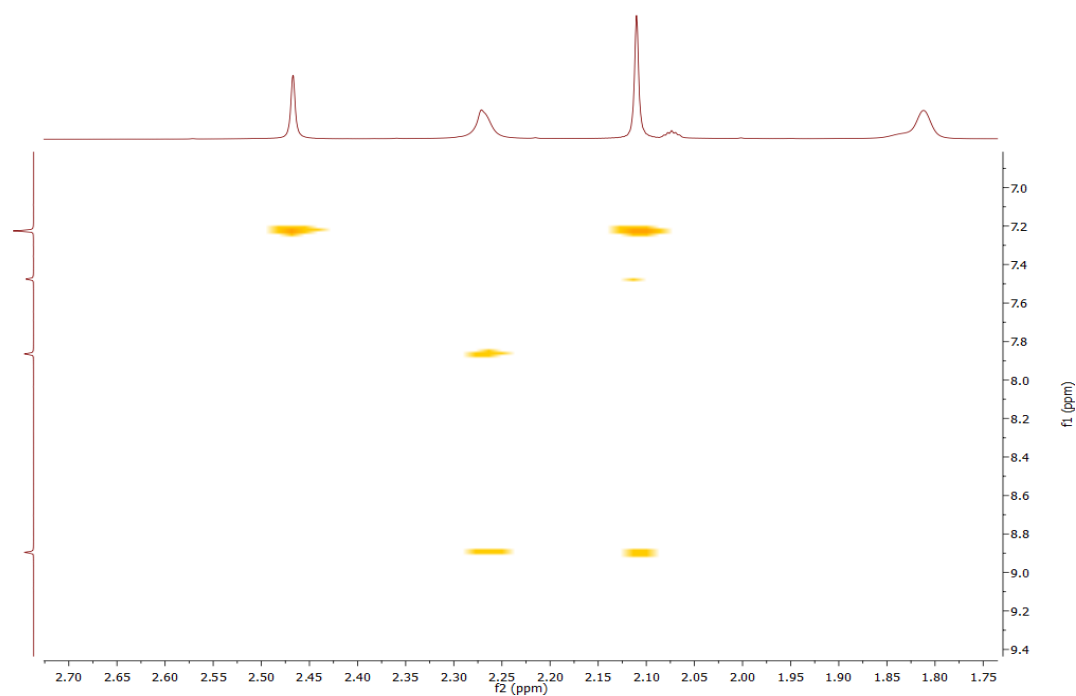


Fig. S5. $^1\text{H}[^{11}\text{B}]$ -NOESY NMR spectrum of **8** with an enlargement of the imidazolium cross-peaks and *ortho* mesityl methyl groups.

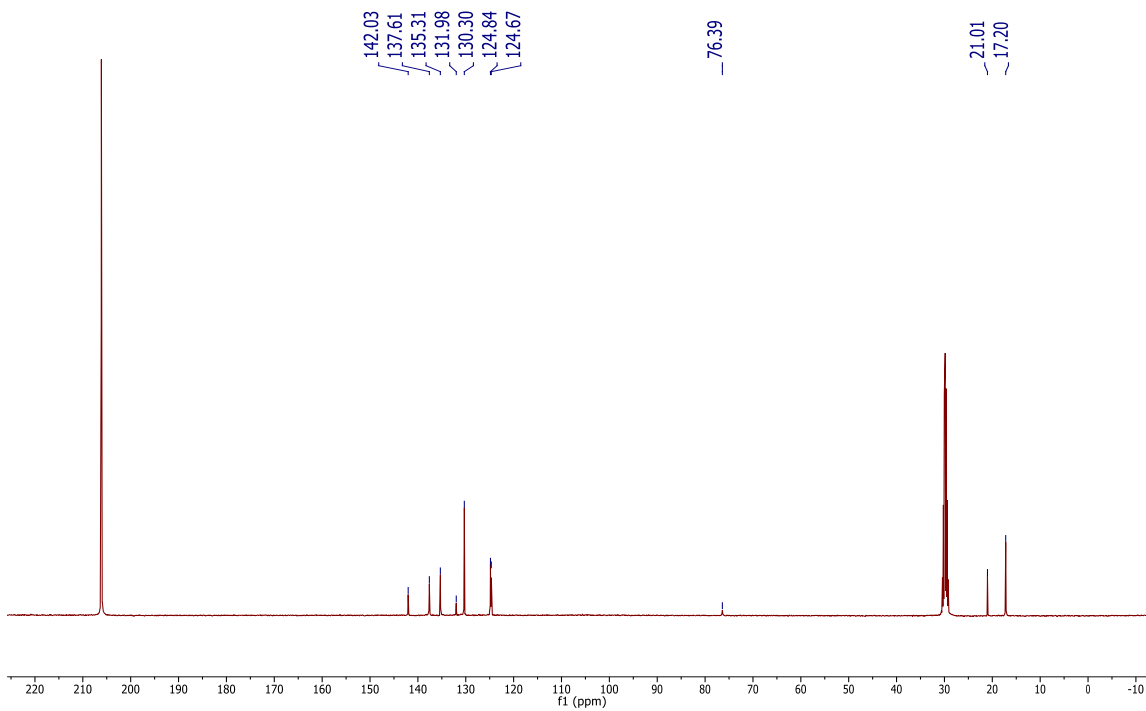


Fig. S6. $^{13}\text{C}[^1\text{H}]$ NMR of **8** in acetone- d_6 .

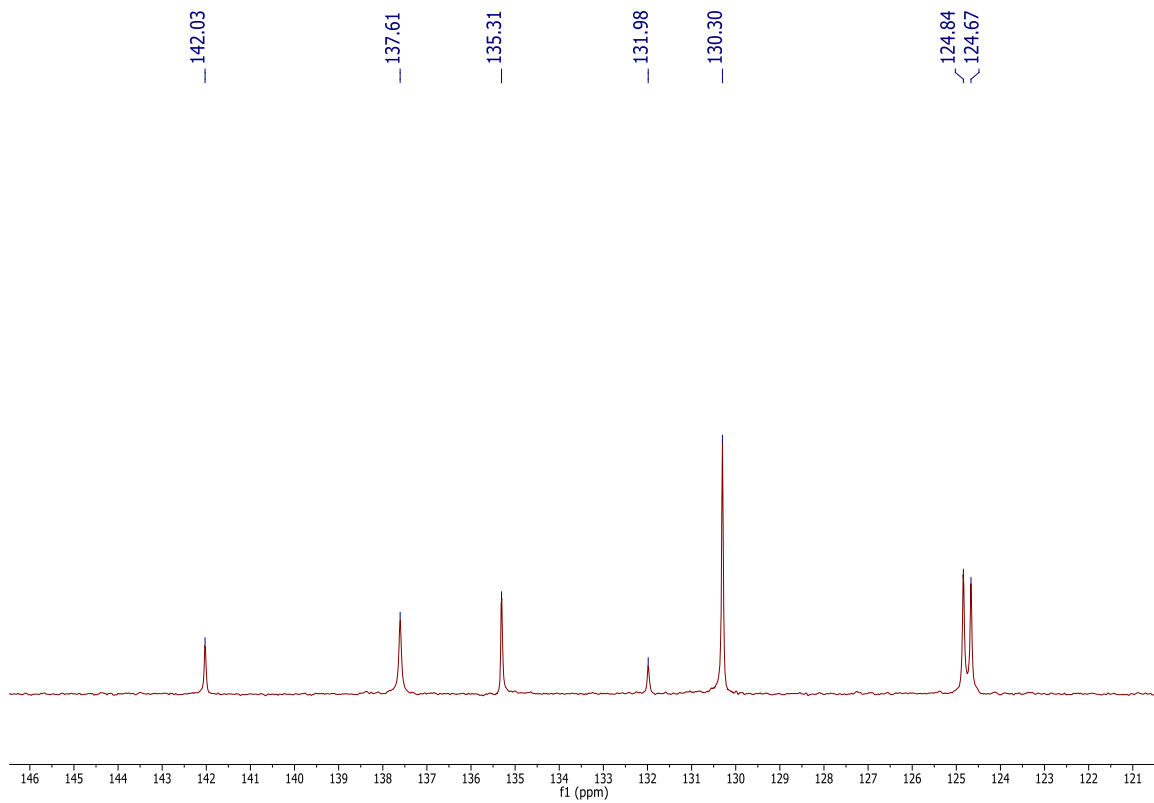


Fig. S7. Detail of the downfield region of the $^{13}\text{C}[^1\text{H}]$ NMR of **8** in acetone- d_6 .

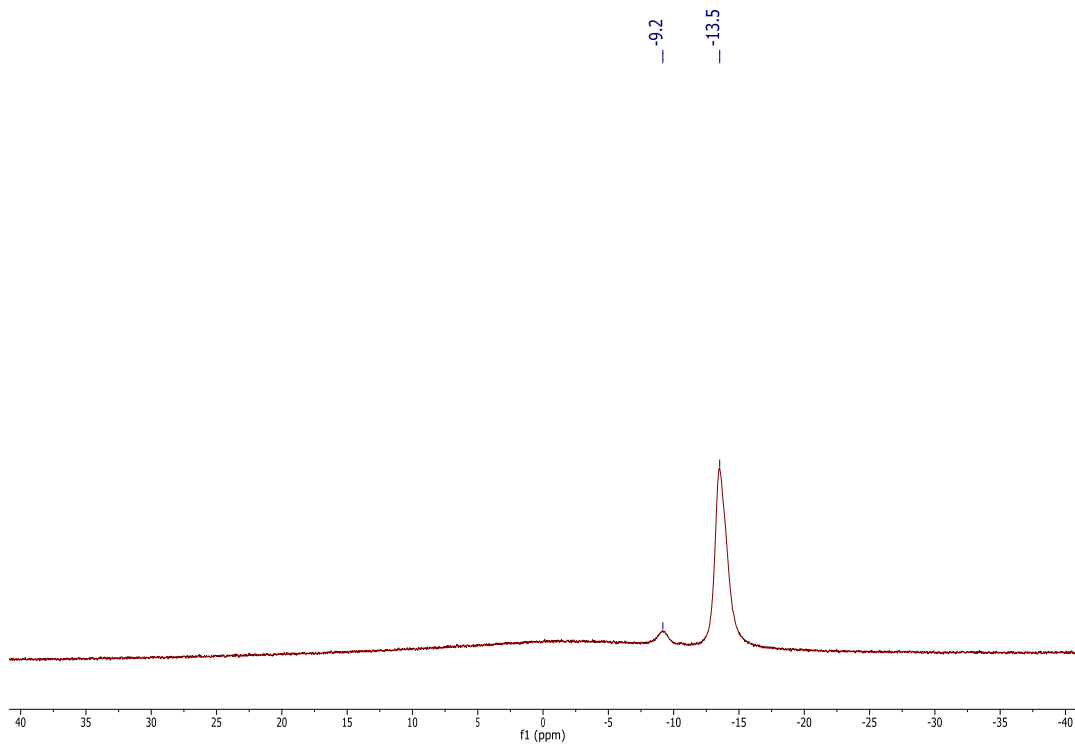


Fig. S8. $^{11}\text{B}[^1\text{H}]$ NMR spectrum of **8** in acetonitrile- d_3 .

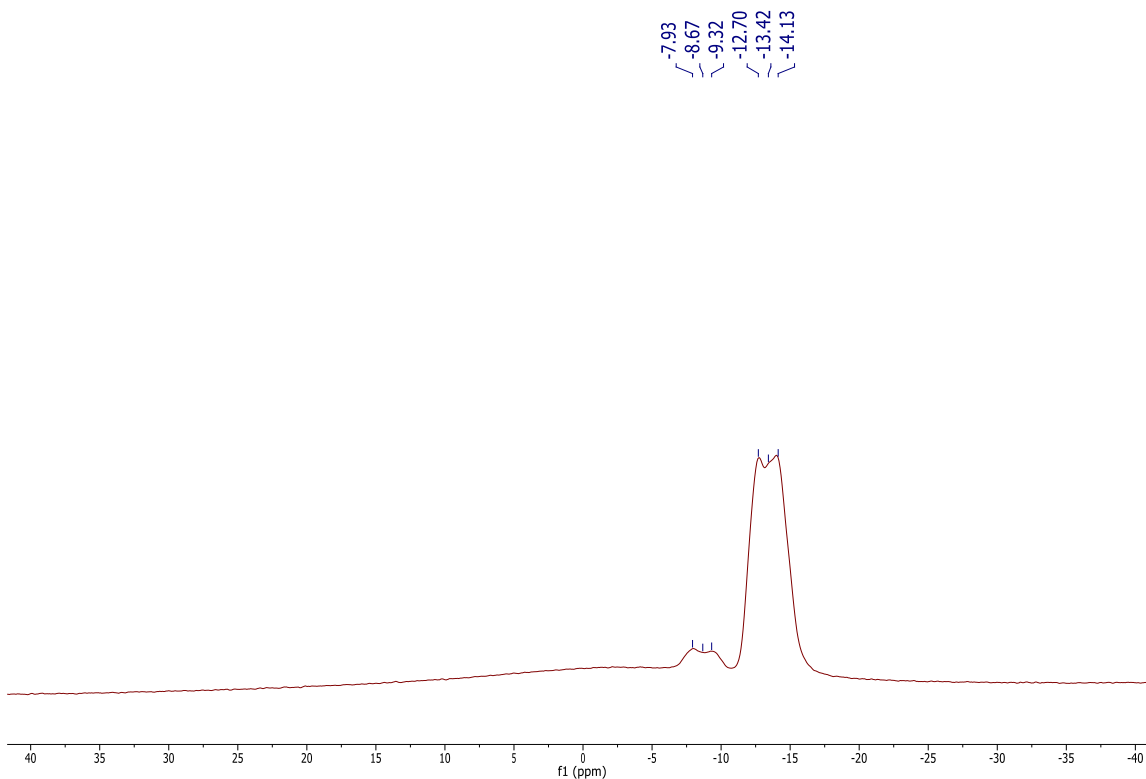


Fig. S9. ^{11}B NMR of **8** in acetonitrile- d_6 showing the ^1J B-H coupling.

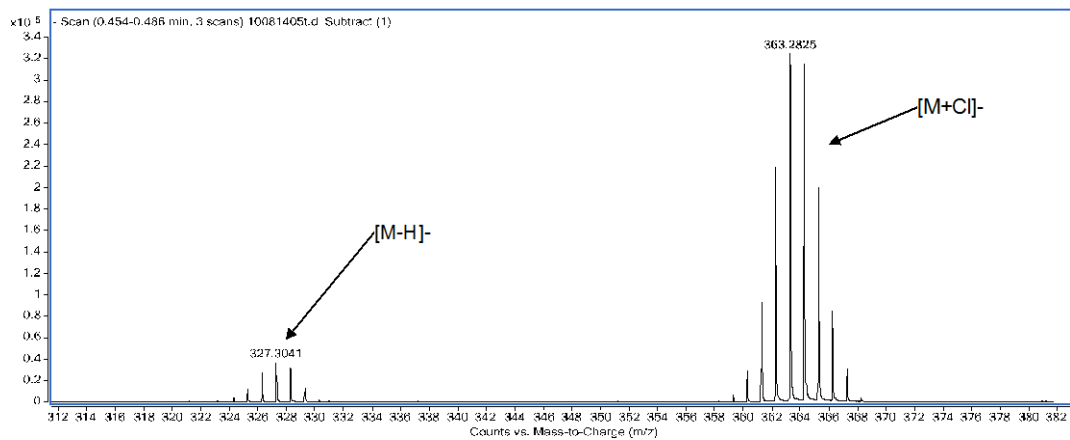


Fig. S10. Mass spectrum (–ve ESI/APC) of **8**. *Note: we always observe a chlorine adduct, presumably formed in flight. $[\text{M}+\text{Cl}]^-$ m/z . Calc: $\text{C}_{13}\text{H}_{25}\text{IOB}_2\text{11B}_9\text{N}_2\text{Cl} = 363.2807$; Found = 363.2825. ppm = 4.7.*

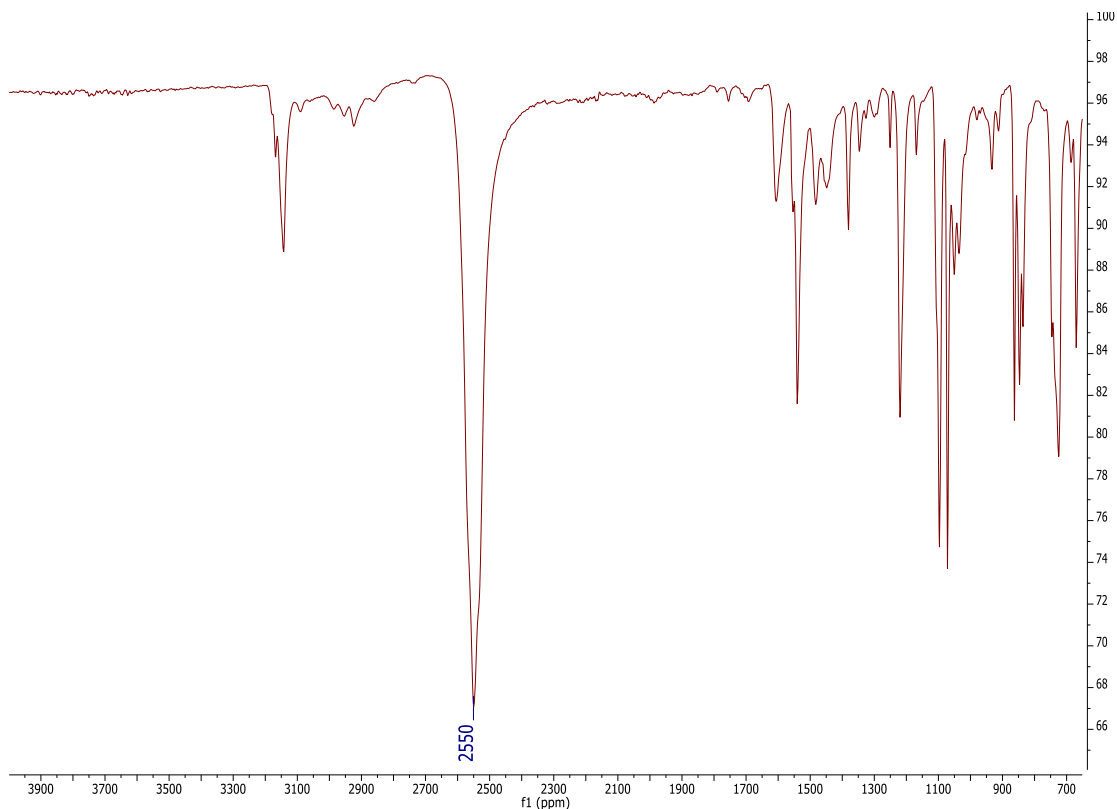
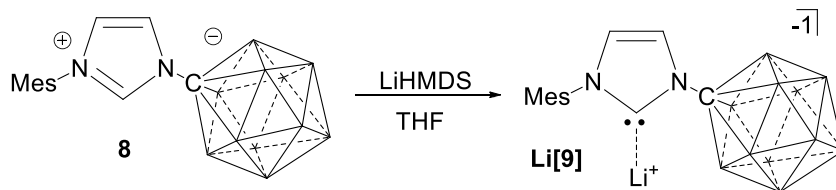


Fig. S11. IR spectrum of solid **8**. The B-H stretches appear at 2550 cm^{-1} .

Synthesis of the monoanionic lithium carbene, Li[9]:



A glass scintillation vial equipped with a stir bar was loaded with **8** (60.0 mg, 0.18 mmol) and lithium hexamethyldisilazide (61.2 mg, 0.37 mmol). THF (1.2 mL) was added to the stirring mixture and allowed to react for one hour. After an hour a yellow-brown precipitate formed and the supernate was carefully removed. The solid was subsequently washed with ether ($3 \times 3\text{ mL}$) and dried in vacuo to furnish the desired compound, **Li[9]** (78.0 mg, 76%). Single crystals of **Li[9]** suitable for X-ray diffraction analysis could be obtained as pale yellow plates from a concentrated THF solution. ^1H NMR (300 MHz, THF- d_8 , 25°C): $\delta = 7.40$ (d, $^3J(\text{H,H}) = 1.5\text{ Hz}$, 1H), 6.98 (s, 2H), 6.79 (d, $^3J(\text{H,H}) = 1.5\text{ Hz}$, 1H), 2.30 (s, 3H), 1.95 (s, 6H), 3.00 – 0.72 (bm, 11H, B-H). $^{13}\text{C}[^1\text{H}]$ NMR (200 MHz, THF- d_8 , 25°C): $\delta = 199.9, 139.2, 139.2, 135.7, 129.6, 123.3, 121.3, 80.9, 20.8, 17.4\text{ ppm}$. $^{11}\text{B}[^1\text{H}]$ NMR (96MHz, THF, 25°C): $\delta = -10.0, -11.3\text{ ppm}$. ^7Li NMR (233 MHz, THF, 25°C) = 2.29 ppm. IR (solid, ATR, 25°C): B-H stretch = 2655, 2557, 2523 cm^{-1} .

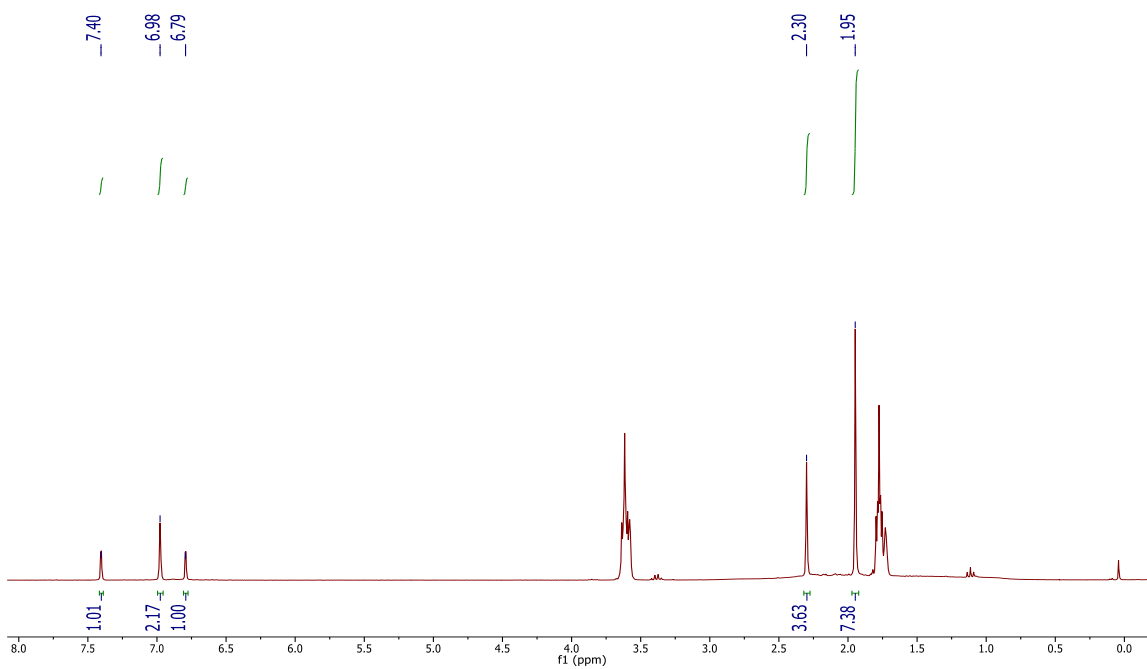


Fig. S12. $^1\text{H-NMR}$ spectrum of **Li[9]** in THF-d_8 . The peak near 0 ppm is due to coordinated HMDS. Traces of diethyl ether can be seen at 3.4 and 1.1 ppm.

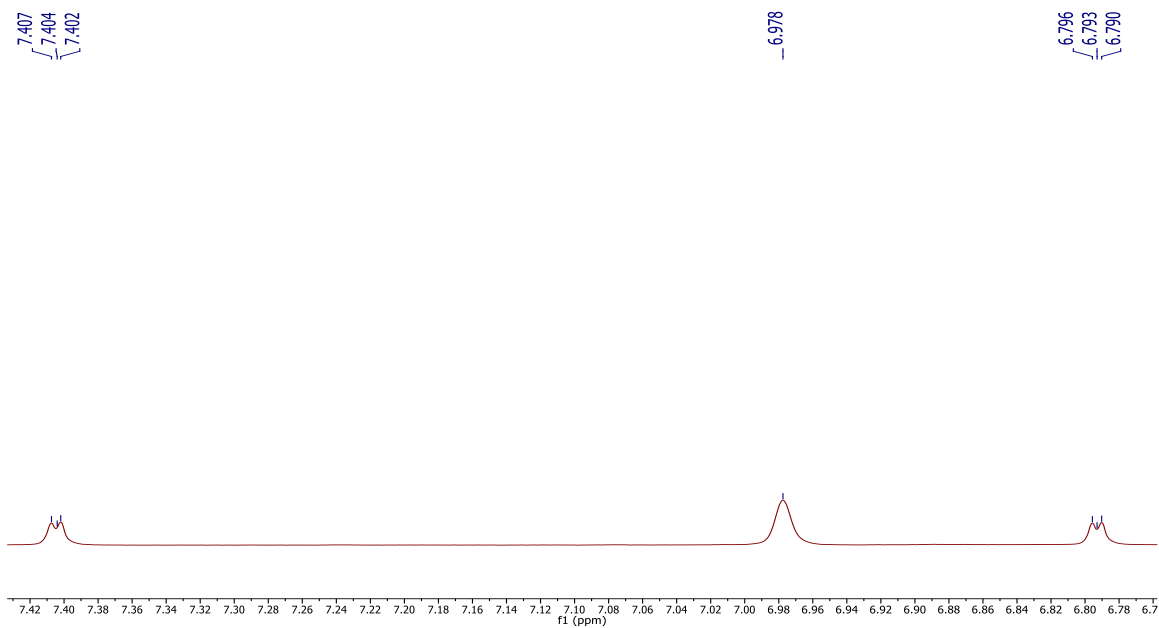


Fig. S13. An expanded view of the aromatic region of the $^1\text{H-NMR}$ of **Li[9]** in THF-d_8 , showing the small 3J -coupling of the imidazolyliidene protons.

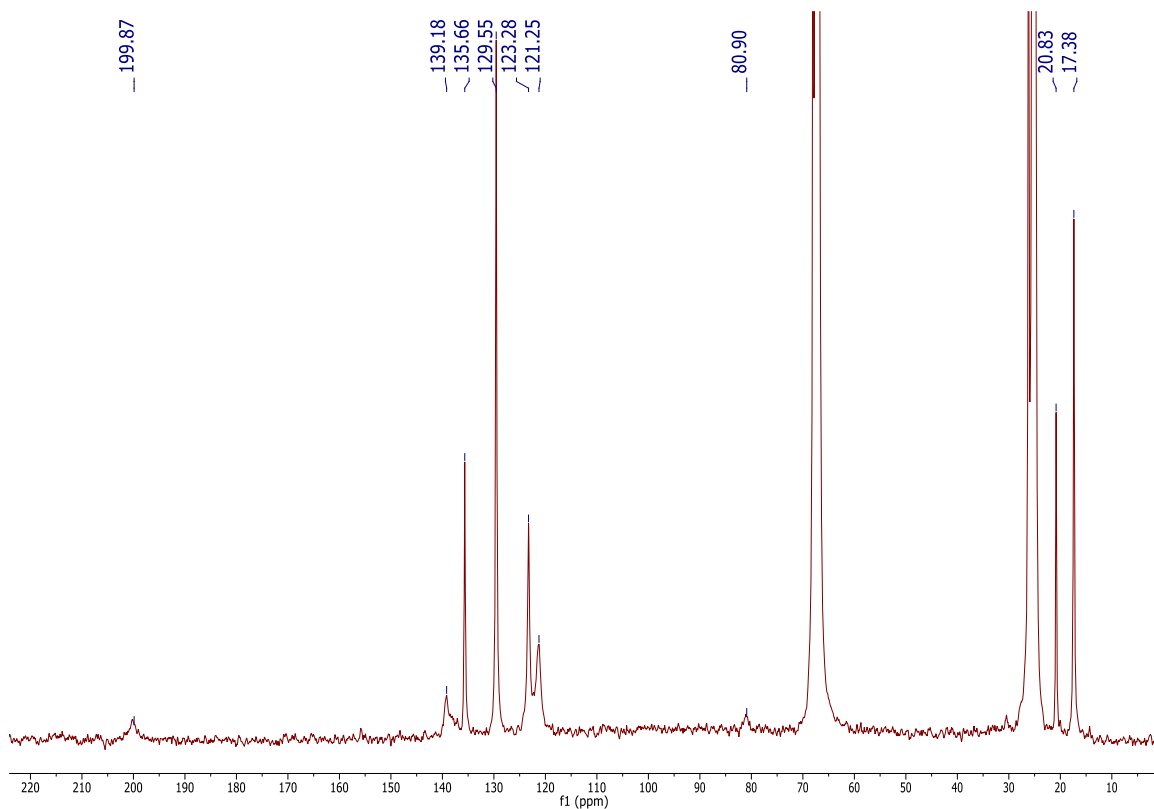


Fig. S14. $^{13}\text{C}\{^1\text{H}\}$ NMR spectrum of **Li[9]** in THF-d_8 .

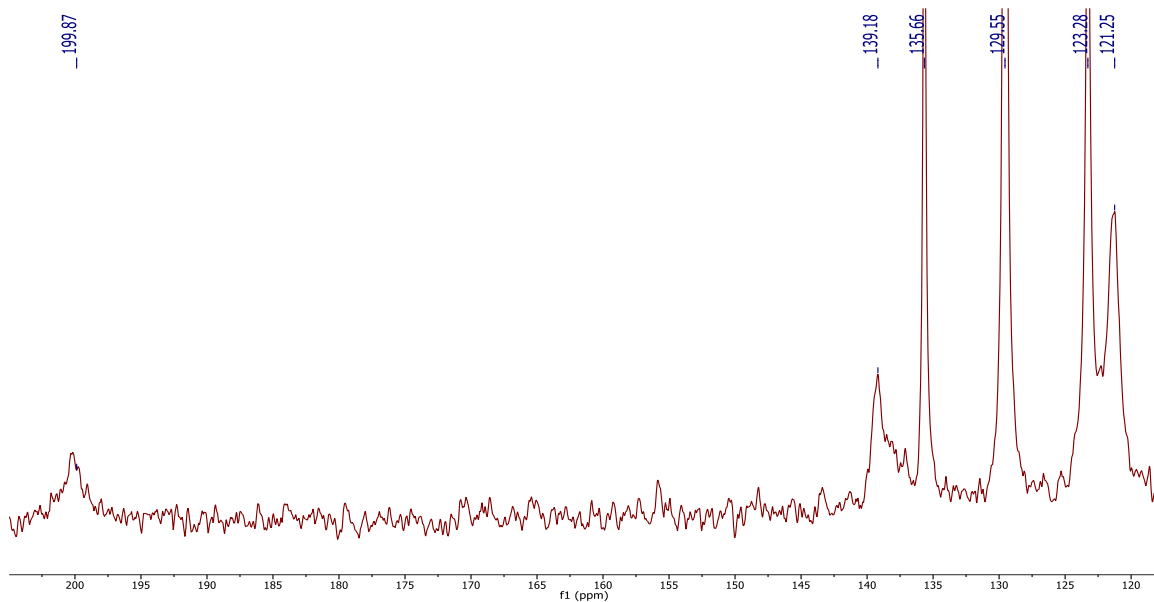


Fig. S15. An expanded view of the downfield region of the $^{13}\text{C}\{^1\text{H}\}$ NMR of **Li[9]** in THF-d_8 . Note: The broad resonance at 139.2 ppm is two superimposed quaternary carbons with in the mesityl-ring.

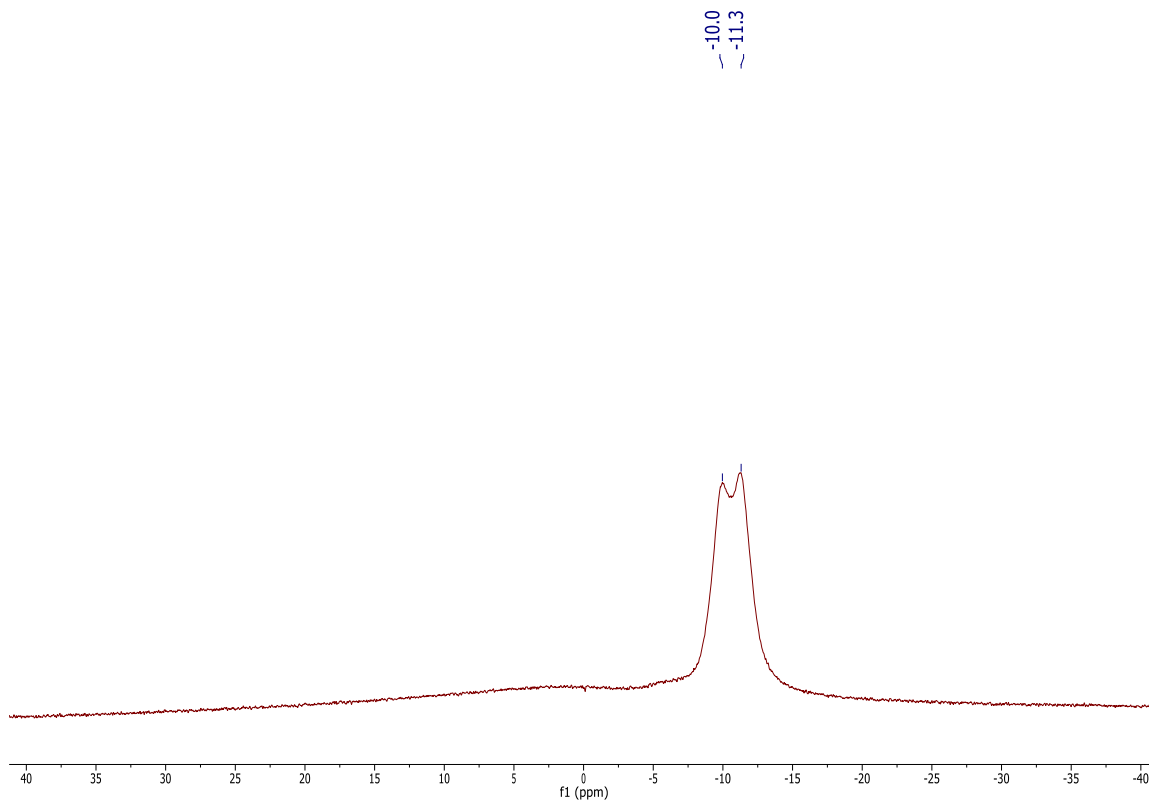


Fig. S16. $^{11}\text{B}[^1\text{H}]$ -NMR spectrum of **Li[9]** in THF.

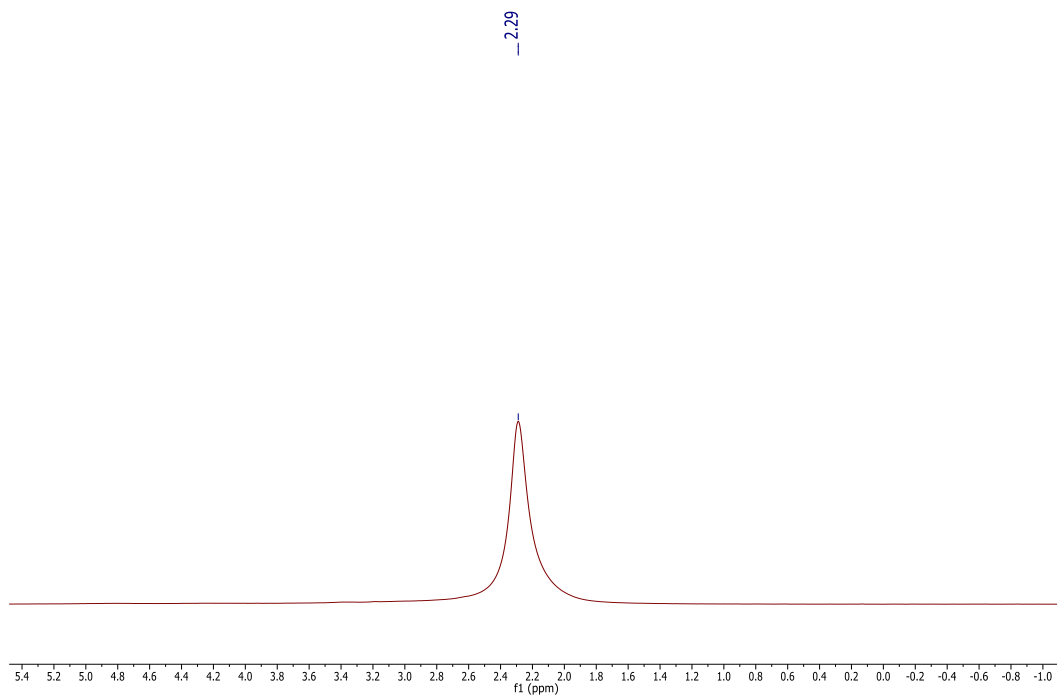


Fig. S17. ^7Li -NMR spectrum of **Li[9]** in THF.

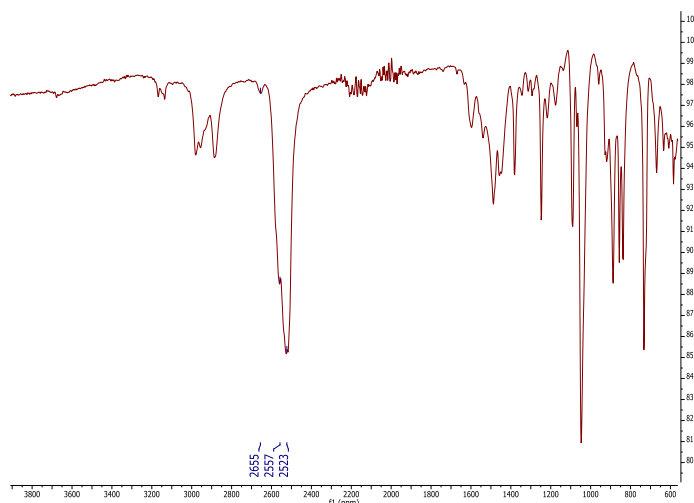
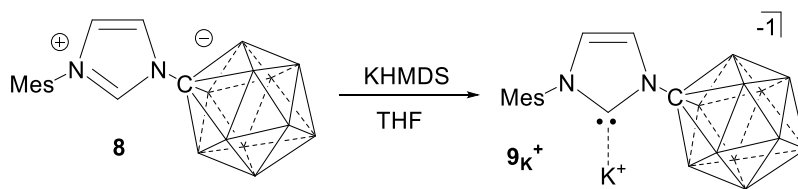


Fig. S18. IR spectrum of solid **Li[9]**. The B-H stretches at 2655, 2557 and 2523 cm^{-1} .

Synthesis of the monoanionic potassium carbene, **K[9]:**



A vial was equip with a stir bar and loaded with **8** (1.23 g, 3.75 mmol) and KHMDS (0.63 g, 5.61 mmol). THF (5 mL) was added to dissolve the stirring solids. After 1h the mixture was filtered and crystallized by adding diethyl ether (2 mL). Light brown cubes of **K[9]**•(THF)_{2.5}(ether)_{3.0} formed at -30°C . (1.24 g, 61%). ^1H NMR (300 MHz, benzene- d_6 , 25°C): δ = 7.29 (d, $^3J(\text{H,H})$ = 1.8 Hz, 1H), 6.66 (s, 2H), 5.85 (d, $^3J(\text{H,H})$ = 1.8 Hz, 1H), 2.10 (s, 3H), 1.72 (s, 6H), 3.87-1.00 (bm, 11H, B-H). $^1\text{H}[^{11}\text{B}]$ NMR (96 MHz, benzene- d_6 , 25°C): δ = 7.29 (1H), 6.65 (2H), 5.85 (1H), 2.75 (5H), 2.34 (5H), 2.10 (3H), 2.01 (5), 1.73 (6H) ppm. ^1H NMR (400 MHz, THF- d_8 , 25°C): δ = 7.35 (d, $^3J(\text{H,H})$ = 1.6 Hz, 1H), 6.96 (s, 2H), 6.70 (d, $^3J(\text{H,H})$ = 1.6 Hz, 1H), 2.29 (s, 3H), 1.94 (s, 6H), 2.88-0.84 (bm, 11H, B-H). $^1\text{H}[^{11}\text{B}]$ NMR (96 MHz, THF- d_8 , 25°C): δ = 7.34 (1H), 6.95 (2H), 6.70 (1H), 2.29 (3H), 2.13 (5H), 1.94 (6H), 1.63 (5H) ppm. $^{13}\text{C}[^1\text{H}]$ NMR (100 MHz, THF- d_8 , 25°C): δ = 211.3, 139.0, 138.1, 135.7, 129.4, 121.6, 113.0, 82.0, 20.9, 12.6. $^{11}\text{B}[^1\text{H}]$ NMR (96 MHz, THF- d_8 , 25°C): δ = -9.9, -13.9 ppm. ^{11}B NMR (96 MHz, THF- d_8 , 25°C): δ = -9.4 ($^1J(\text{H,B})$ = 129.6 Hz), -13.6 ($^1J(\text{H,B})$ = 141.1 Hz) ppm. IR (solid, ATR, 25°C): B-H stretch = 2670, 2567, 2535 cm^{-1} . m.p. = 62.4 to 63.4 $^{\circ}\text{C}$.

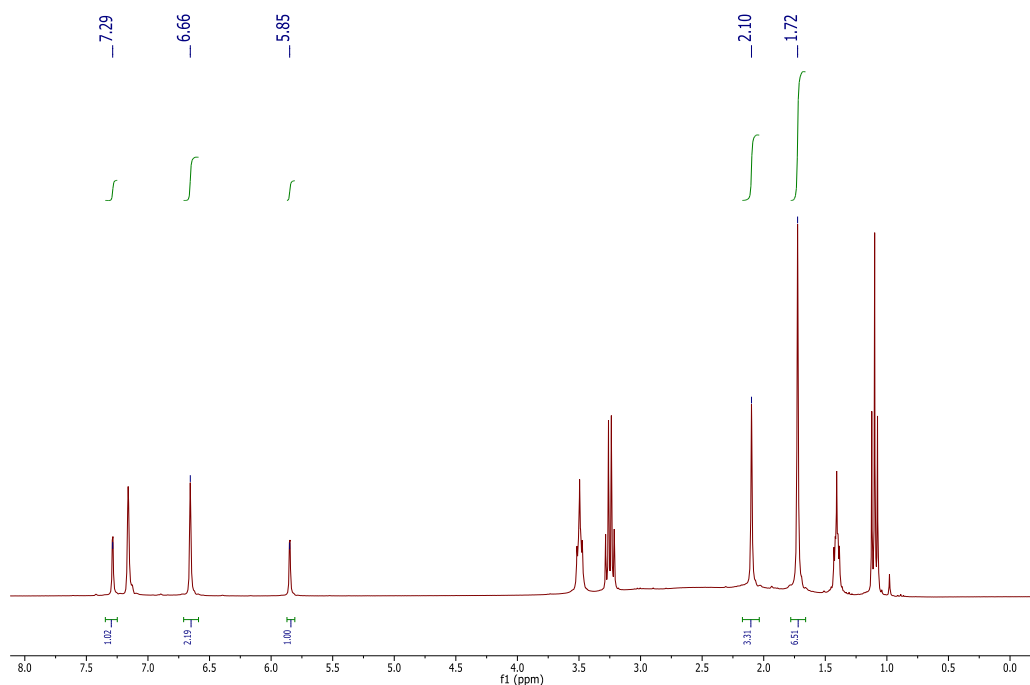


Fig. S19. ^1H -NMR of **K[9]** in benzene- d_6 . Liberated solvents: 2.5 THF and 3.0 Et $_2$ O. Note: we hypothesize that the imidazolylidene ring and mesityl protons of **K[9]** are shifted upfield relative to its ^1H spectrum in D-THF (see Figs S20-22), because of solvation effects induced by the low polarity benzene- d_6 solvent.

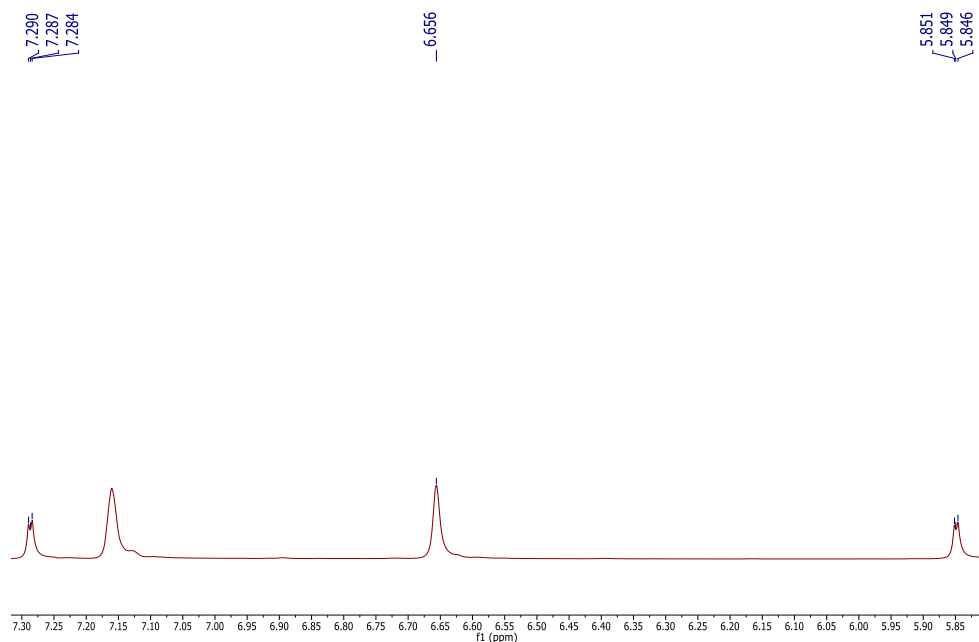


Fig. S20. An expanded view of the aromatic region of the ^1H -NMR of **K[9]** in benzene- d_6 , showing the small 3J -coupling of the imidazolylidene protons.

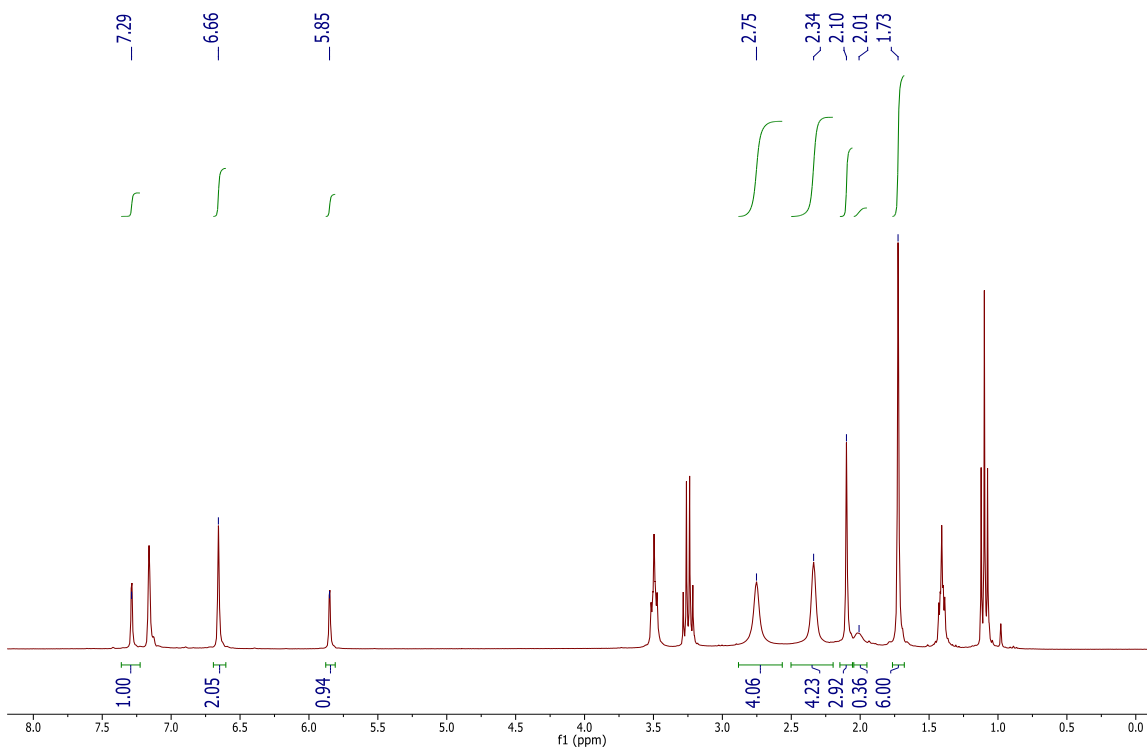


Fig. S21. $^1\text{H}[^{11}\text{B}]$ -NMR spectrum of **K[9]** in benzene- d_6 . The boron hydrides appear at 2.75, 2.34 and 2.01 ppm.

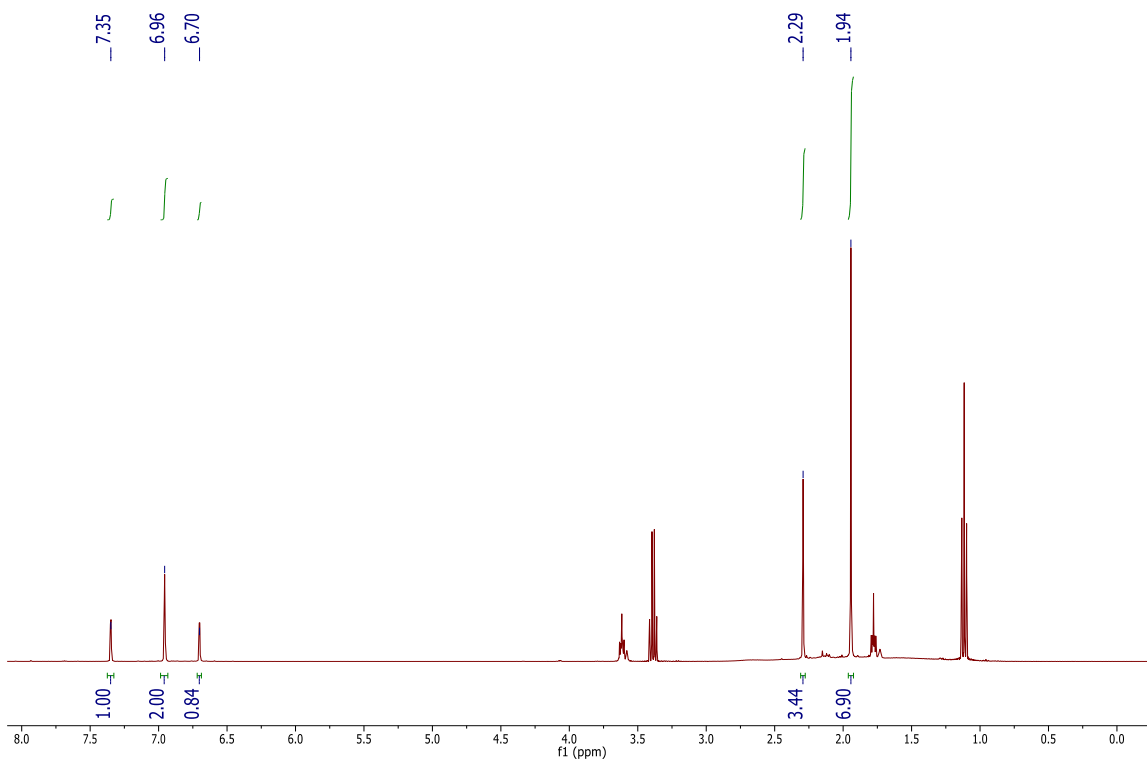


Fig. S22. ^1H -NMR spectrum of **K[9]** in THF- d_8 . Liberated solvents: 1.5 Et $_2$ O.

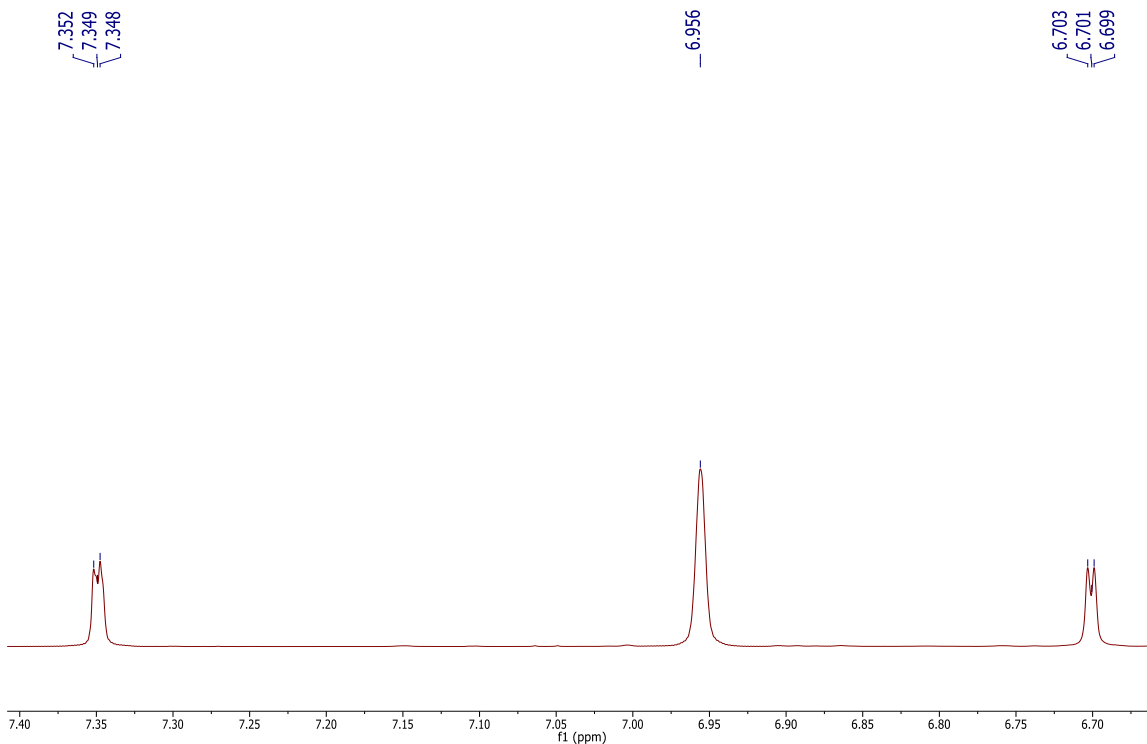


Fig. S23. An expanded view of the aromatic region of the ^1H -NMR of **K[9]** in THF-d_8 , showing the small 3J -coupling of the imidazolylidene protons.

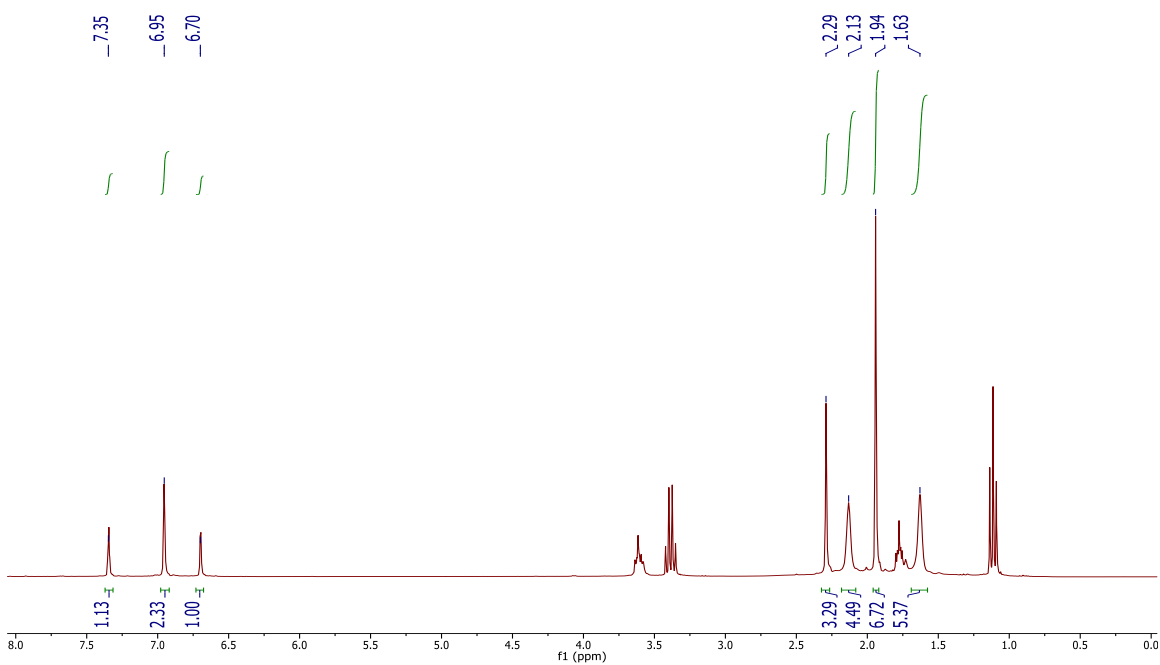


Fig. S24. $^1\text{H}[^{11}\text{B}]$ NMR spectrum of **K[9]** in THF-d_8 . The boron hydrides appear at 2.13 and 1.63 ppm.

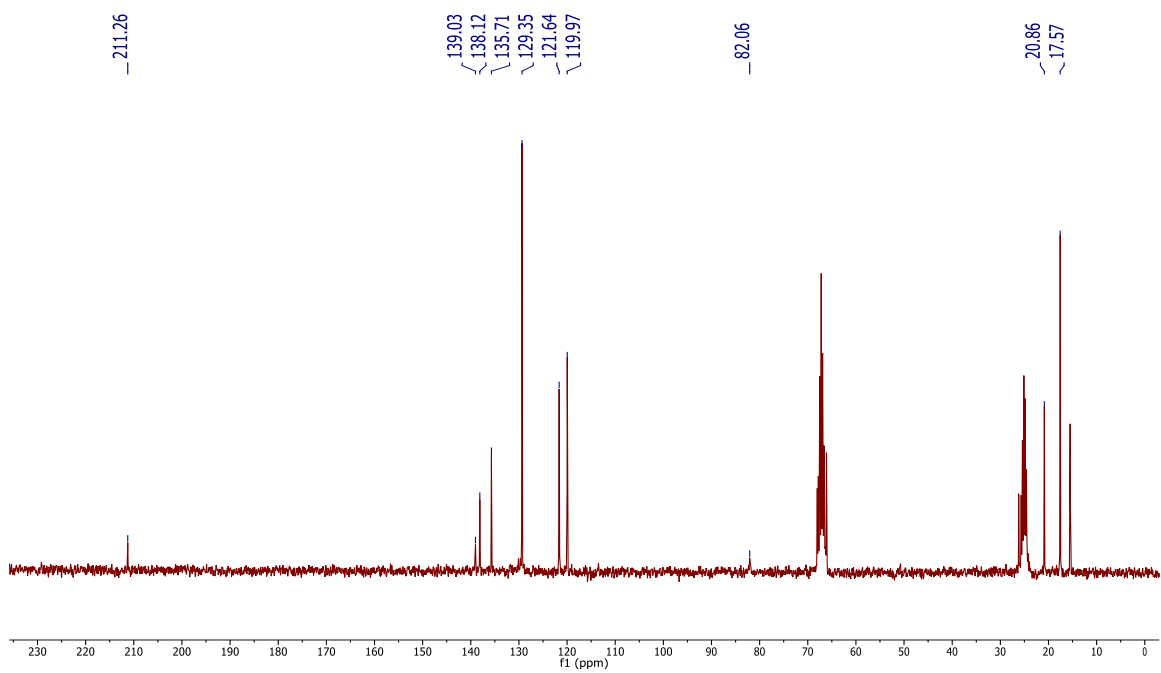


Fig. S25. $^{13}\text{C}[^1\text{H}]$ -NMR of **K[9]** in THF- d_8 . Liberated diethyl ether appears at 15.50 and 66.12 ppm.

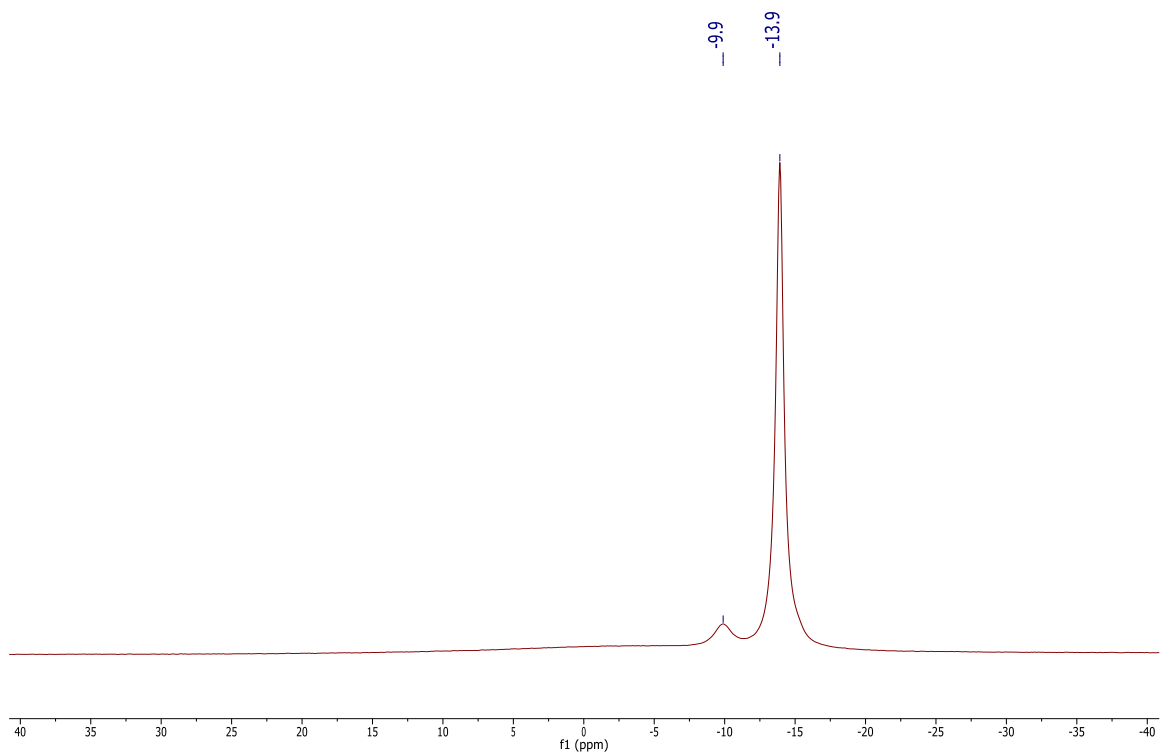


Fig. S26. $^{11}\text{B}[^1\text{H}]$ -NMR of **K[9]** in THF- d_8 .

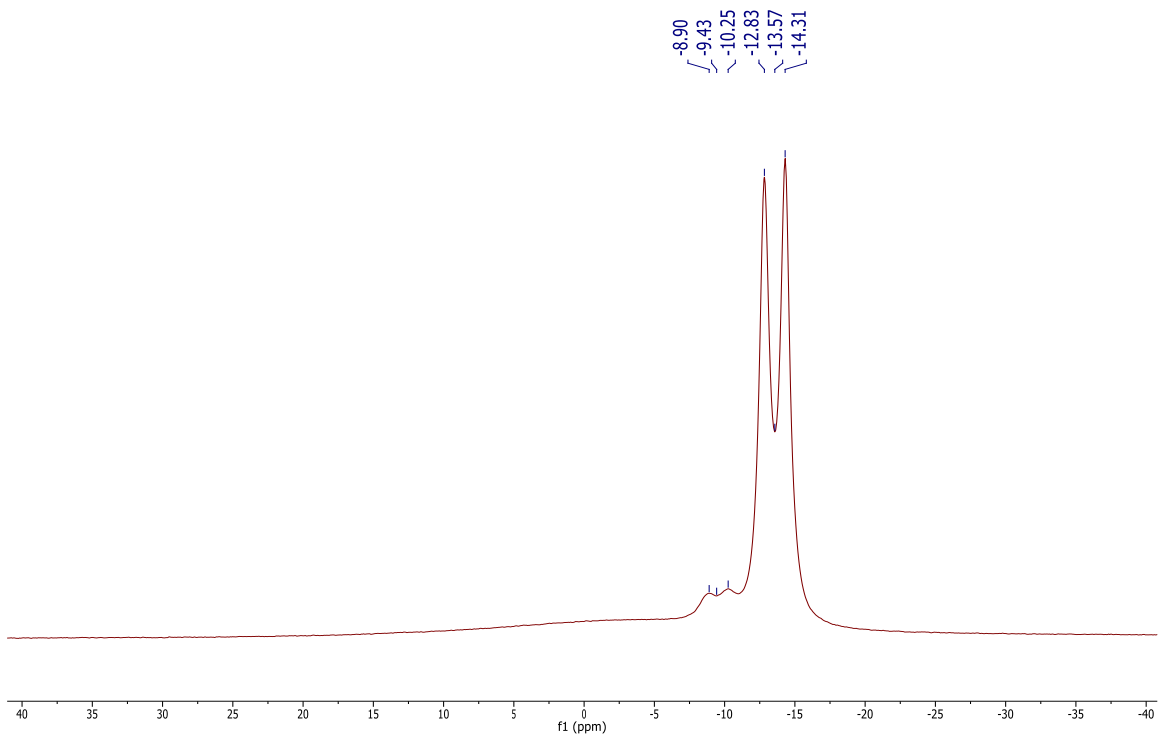


Fig. S27. ^{11}B NMR of **K[9]** in THF-d_8 showing the ^1J B-H coupling.

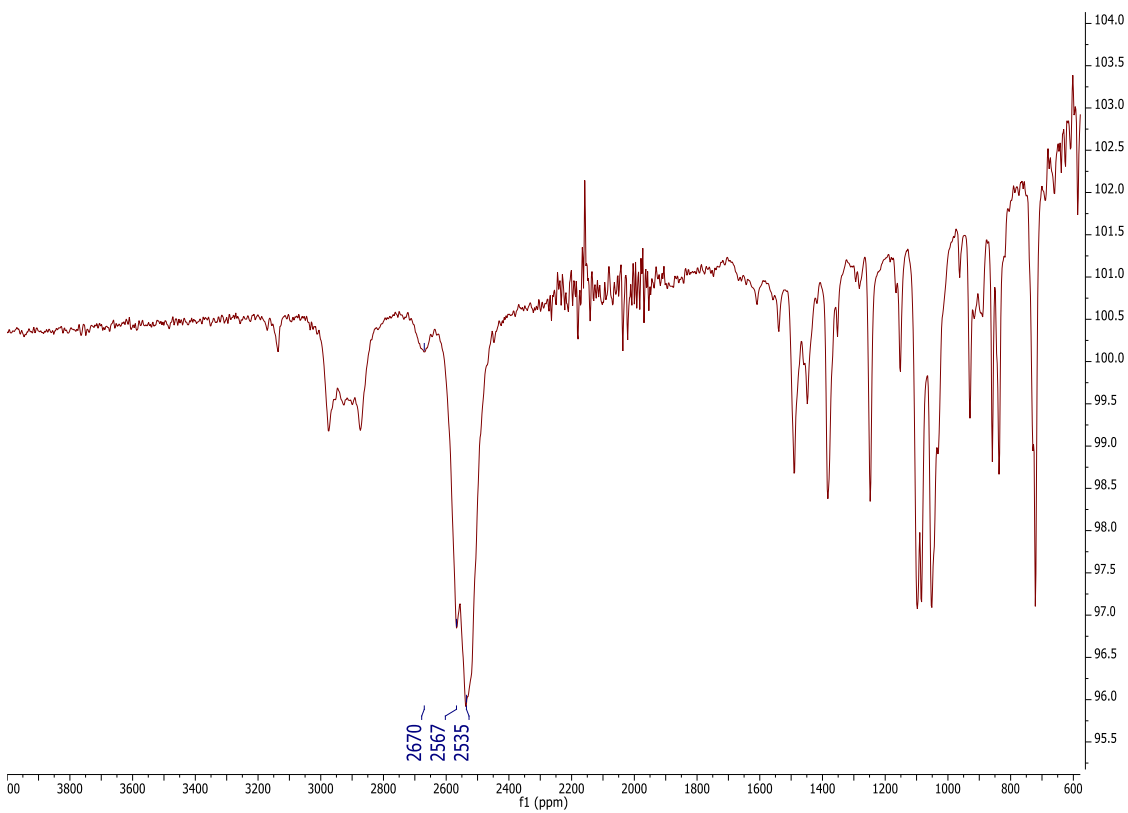
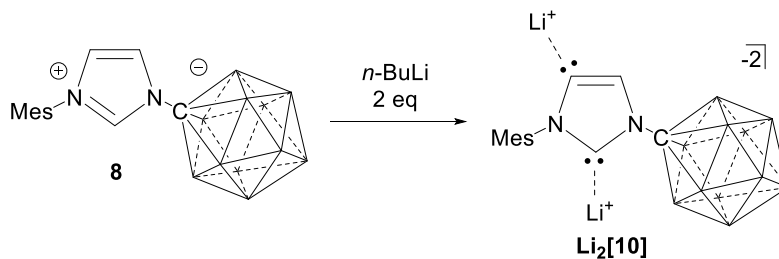


Fig. S28. IR spectrum of solid **K[9]**. The B-H stretches at 2670, 2567 and 2535 cm^{-1} .

Synthesis of the dianionic lithium carbene, $\text{Li}_2[10]$:



To a glass vial equipped with a stir bar was loaded with **8** (296.3 mg, 0.90 mmol) and diethyl ether (17 mL). Next, *n*-butyllithium (1.80 mmol) in ether (2 ml) was added to the stirring suspension of **8**. Following the addition of the *n*-butyllithium an oil began to form along the walls of the vial. The reaction mixture was vigorously stirred and scraped with a spatula periodically over an hour until a yellow solid precipitated from the lime-green solution. The reaction was stirred for another hour and then filtered and washed with diethyl ether. The product, $\text{Li}_2[10] \cdot (\text{Et}_2\text{O})_3$, was collected as a yellow solid (487.4 mg, 96%). Single crystals of $\text{Li}_2[10]$ suitable for X-ray diffraction analysis were grown by layering a concentrated THF solution with diethyl ether. ^1H NMR (400 MHz, THF- d_8 , 25°C): δ = 6.84 (s, 2H), 6.58 (s, 1H), 2.25 (s, 3H), 1.92 (s, 6H), 2.75-0.76 (bm, 11H, B-H). $^1\text{H}[^{11}\text{B}]$ NMR (192.5 MHz, THF- d_8 , 25°C): δ = 6.84 (2H), 6.58 (1H), 2.25 (3H), 2.05 (4H), 1.92 (6H), 1.58 (5H). $^{13}\text{C}[^1\text{H}]$ NMR (100 MHz, THF- d_8 , 25°C): δ = 193.0, 166.8, 145.6, 135.1, 134.5, 127.6, 127.5, 82.1, 20.0, 17.3. $^{11}\text{B}[^1\text{H}]$ NMR (96 MHz, THF- d_8 , 25°C): δ = -10.5, -10.4 ppm. ^{11}B NMR (96 MHz, THF- d_8 , 25°C): δ = -14.2 ($^1J(\text{H},\text{B}) = 130.6$ Hz) ppm. ^7Li NMR (233 MHz, THF- d_8 , 25°C) = 3.54, 2.26 ppm. IR (liquid, THF- d_8 , ATR, 25°C): B-H stretch = 2567, 2542 cm^{-1} . m.p. = 171.1 to 173.4 °C.

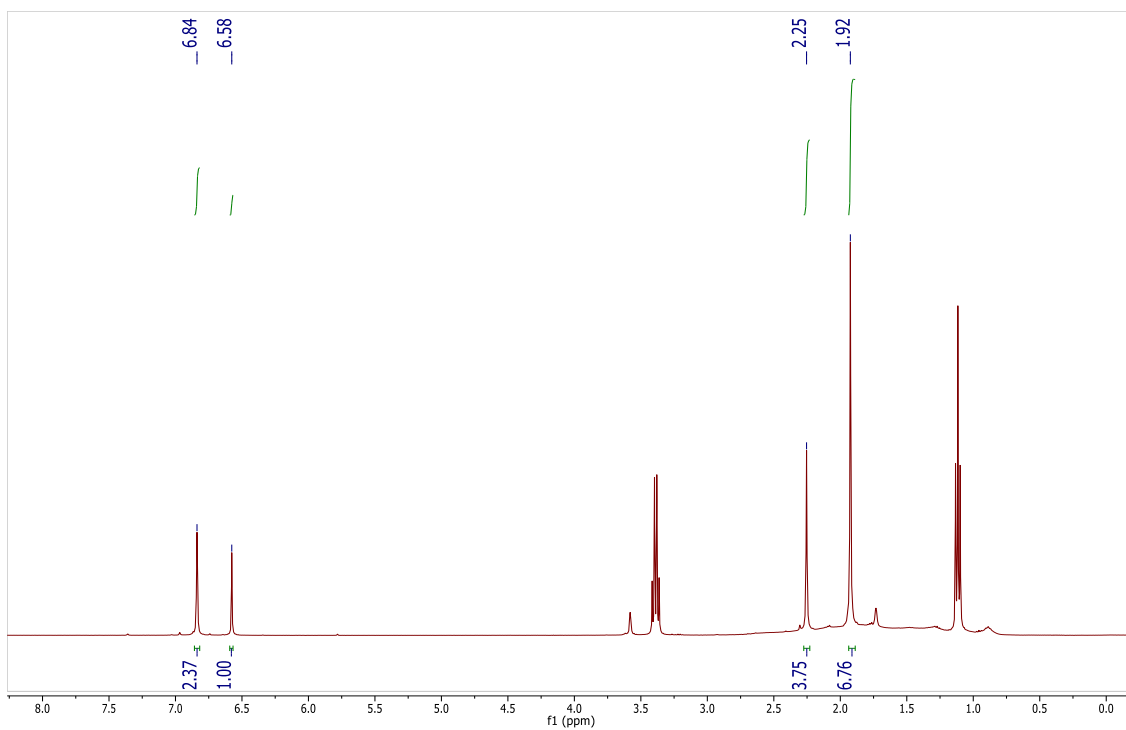


Fig. S29. ^1H -NMR of $\text{Li}_2[10]$ in THF-d_8 . Liberated solvent: 3 Et_2O .

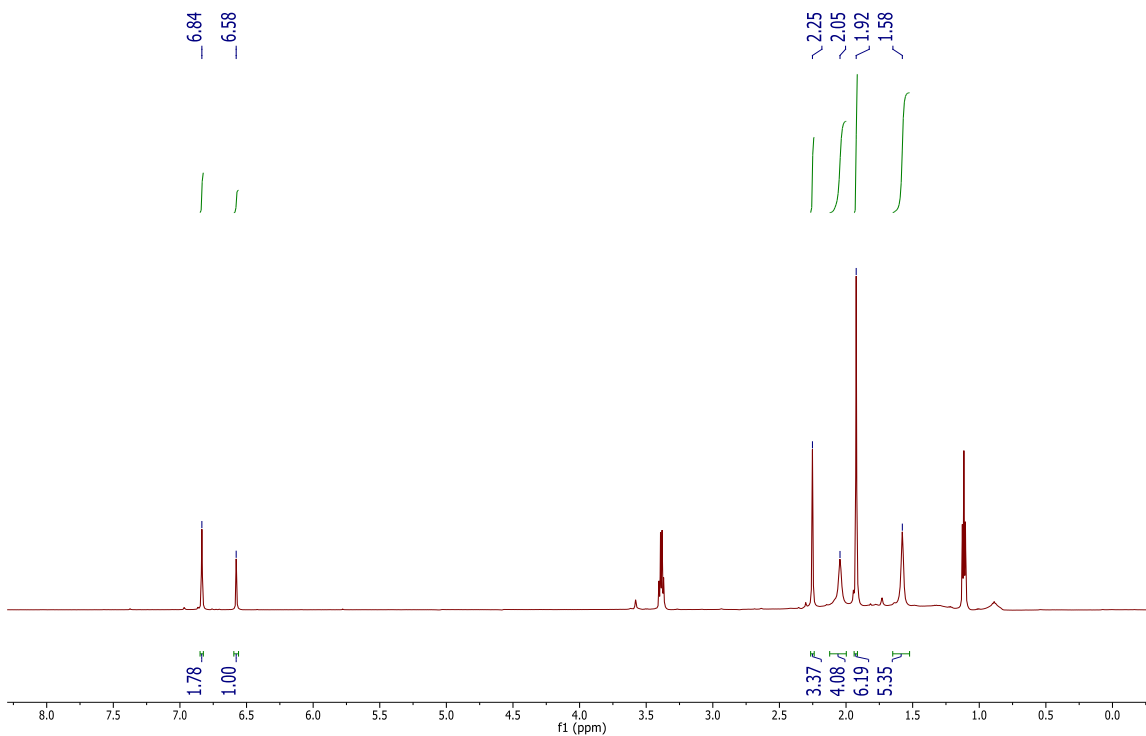


Fig. S30. $^1\text{H}[^{11}\text{B}]$ NMR of $\text{Li}_2[10]$ in THF-d_8 . The boron hydrides can be seen at 2.05 and 1.58 ppm.

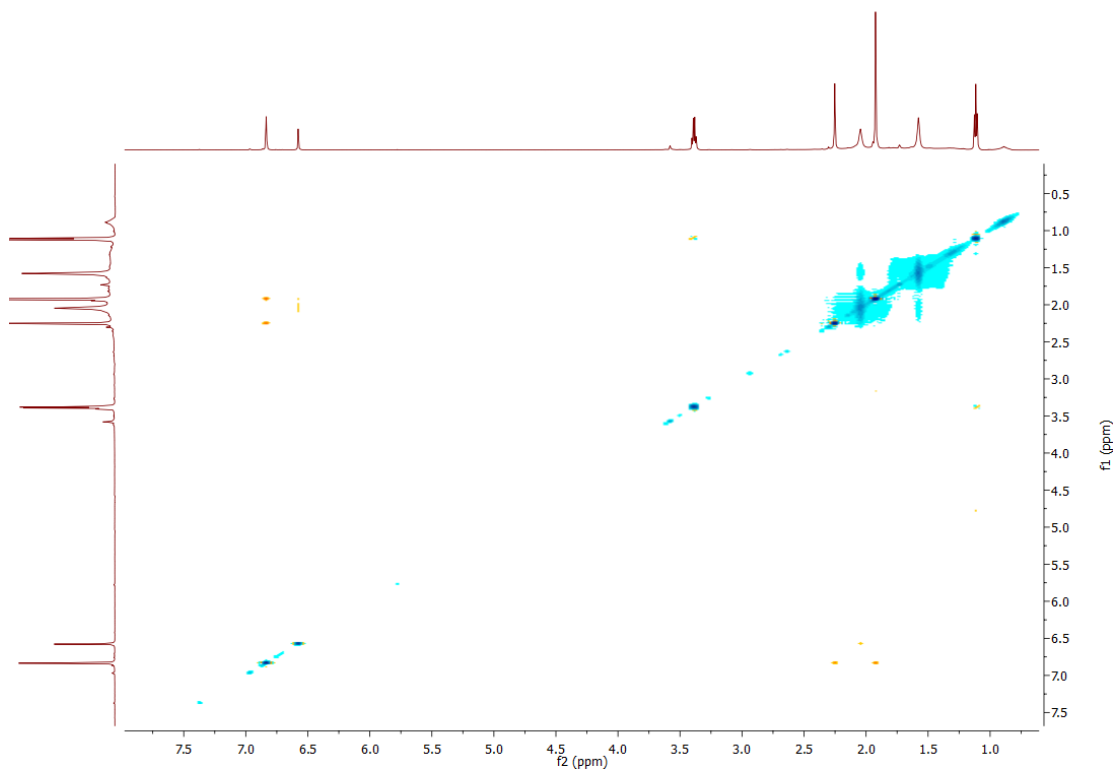


Fig. S31. $^1\text{H}[^{11}\text{B}]$ -NOESY NMR of $\text{Li}_2[10]$ in THF-d_8 , mixing time = 500 ms.

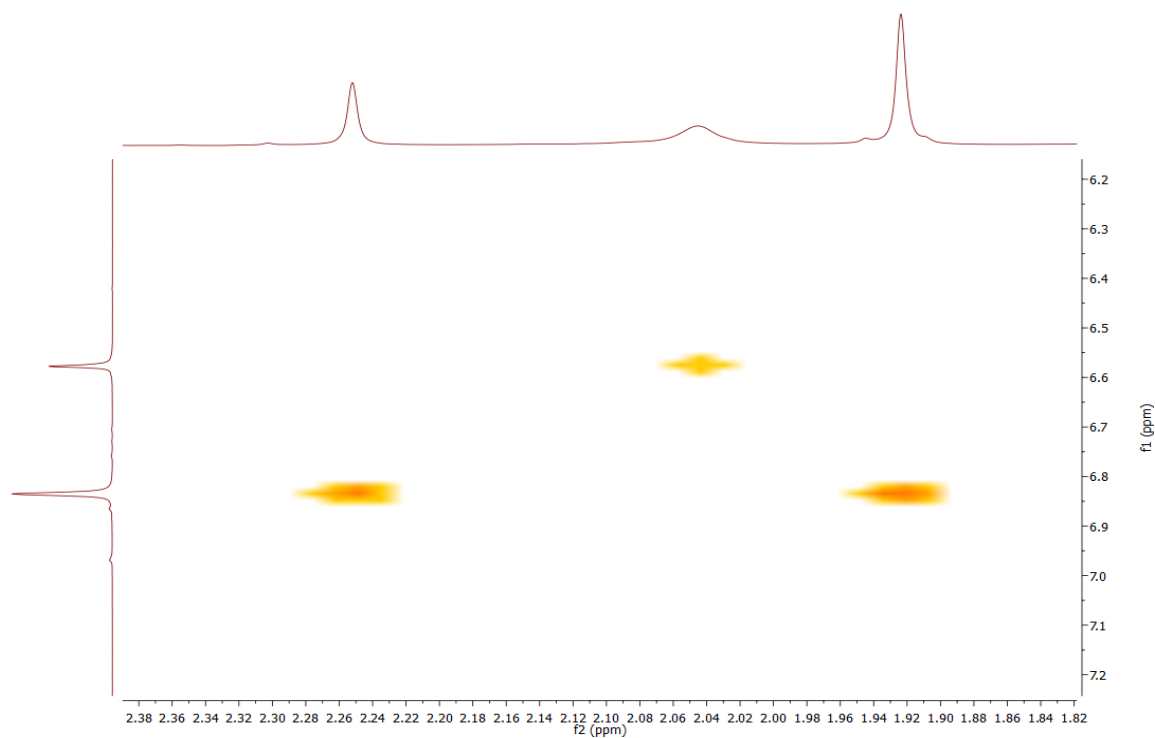


Fig. S32. $^1\text{H}[^{11}\text{B}]$ -NOESY NMR of $\text{Li}_2[10]$ in THF-d_8 , close up of the imidazolylidene cross-peaks.

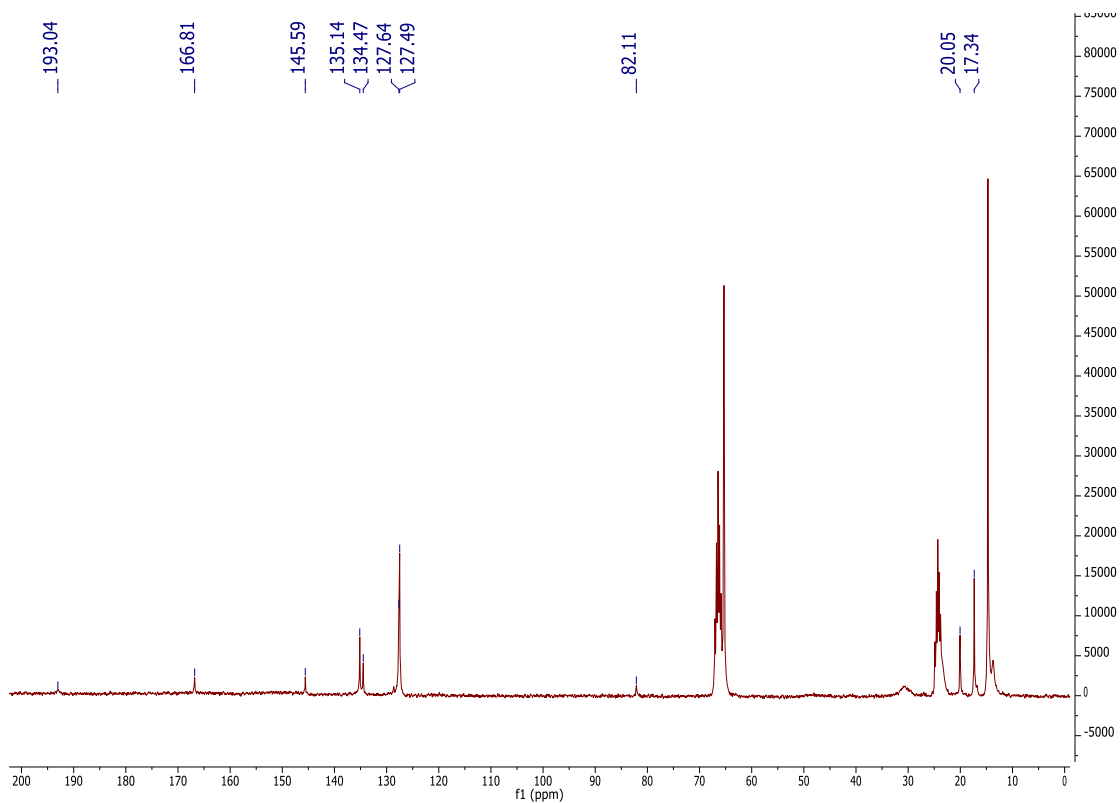


Fig. S33. ^{13}C [^1H] NMR of $\text{Li}_2[10]$ in THF-d_8 . Liberated Et_2O appears at 65.31 and 14.70 ppm.

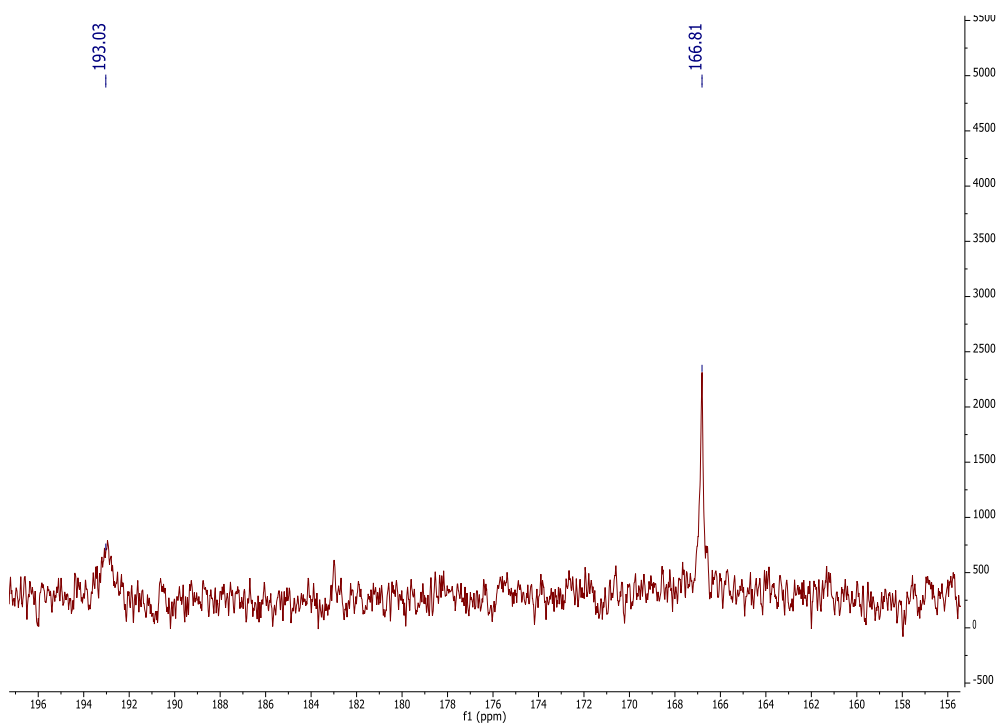


Fig. S34. An expanded view of the lower region of the ^{13}C -NMR of $\text{Li}_2[10]$ in THF-d_8 .

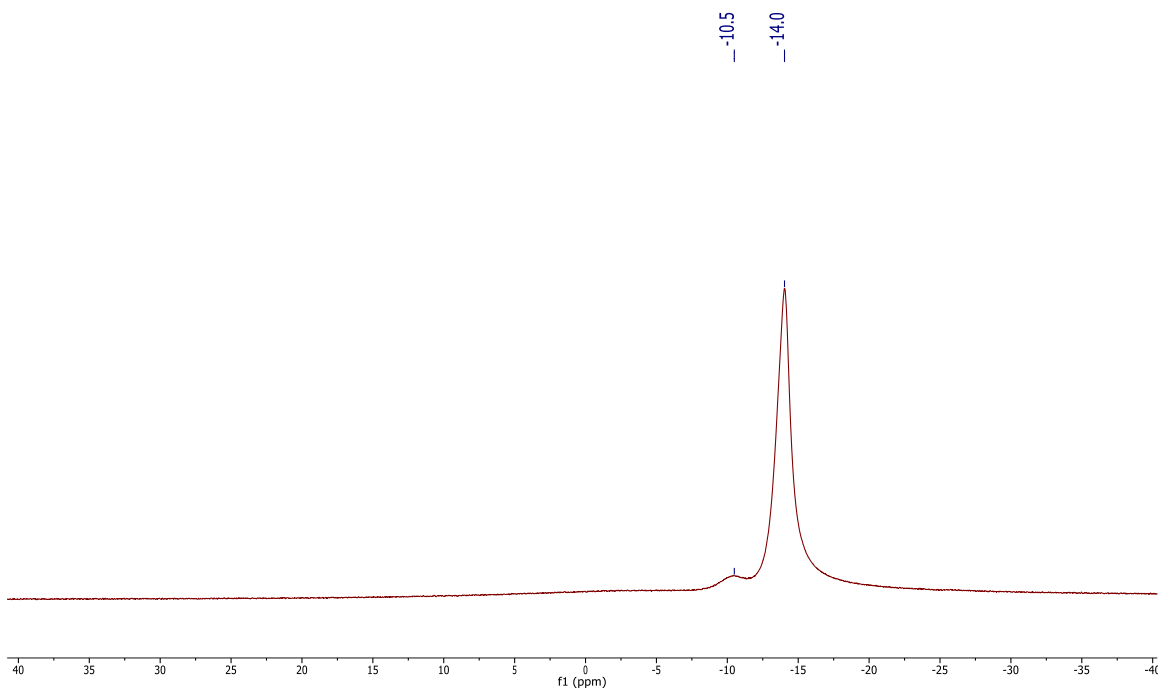


Fig. S35. $^{11}\text{B}[^1\text{H}]$ NMR of $\text{Li}_2[10]$ in THF-d_8 .

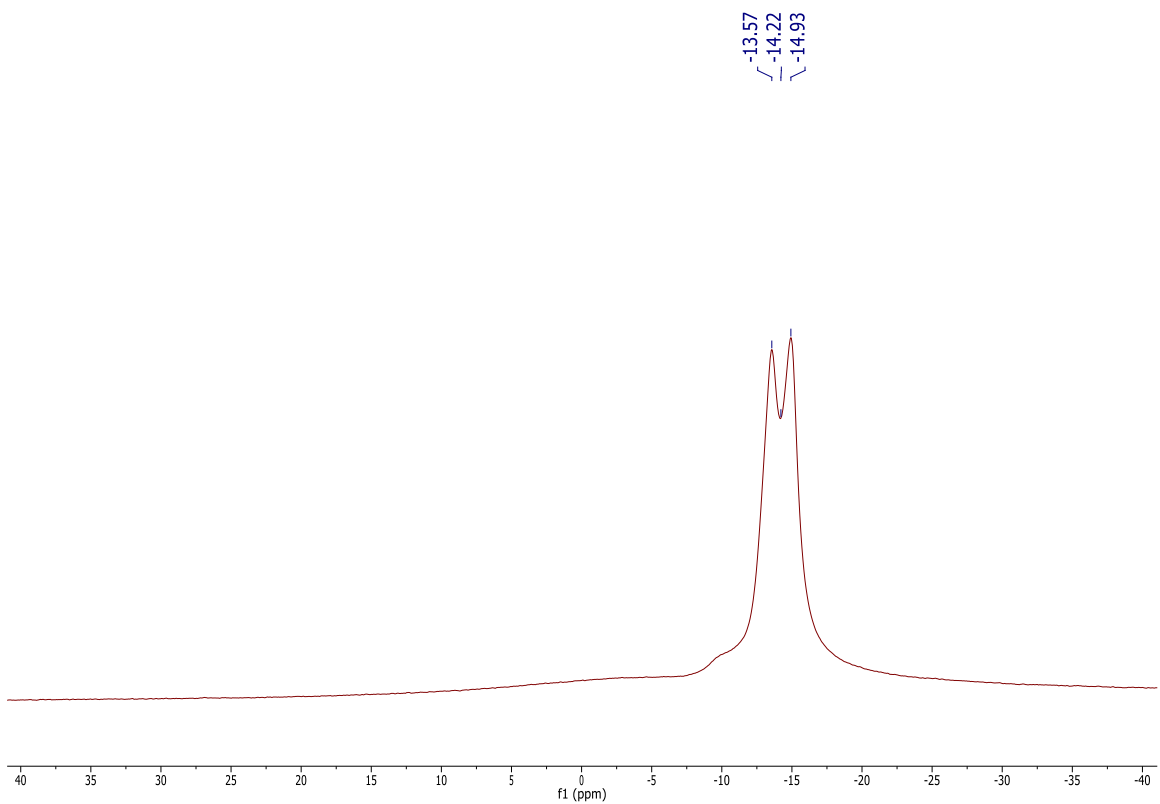


Fig. S36. ^{11}B NMR of $\text{Li}_2[10]$ in THF-d_8 showing the ^1J B-H coupling.

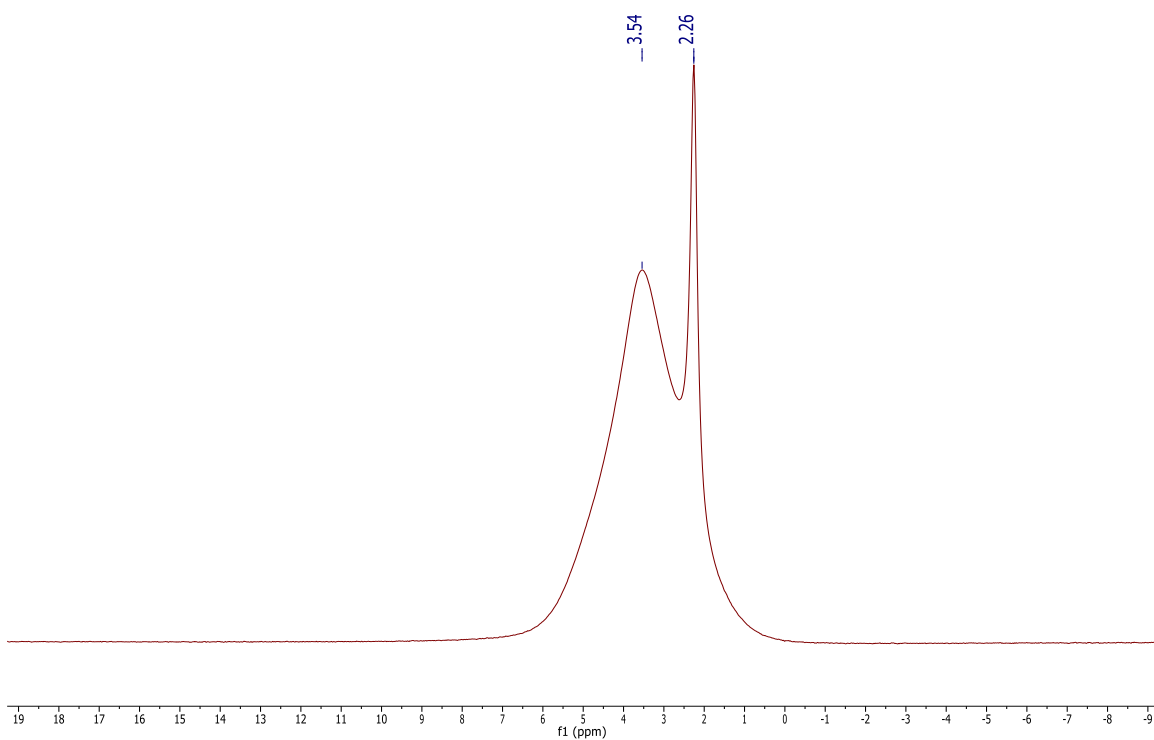


Fig. S37. ^7Li -NMR of $\text{Li}_2[10]$ in THF-d_8 .

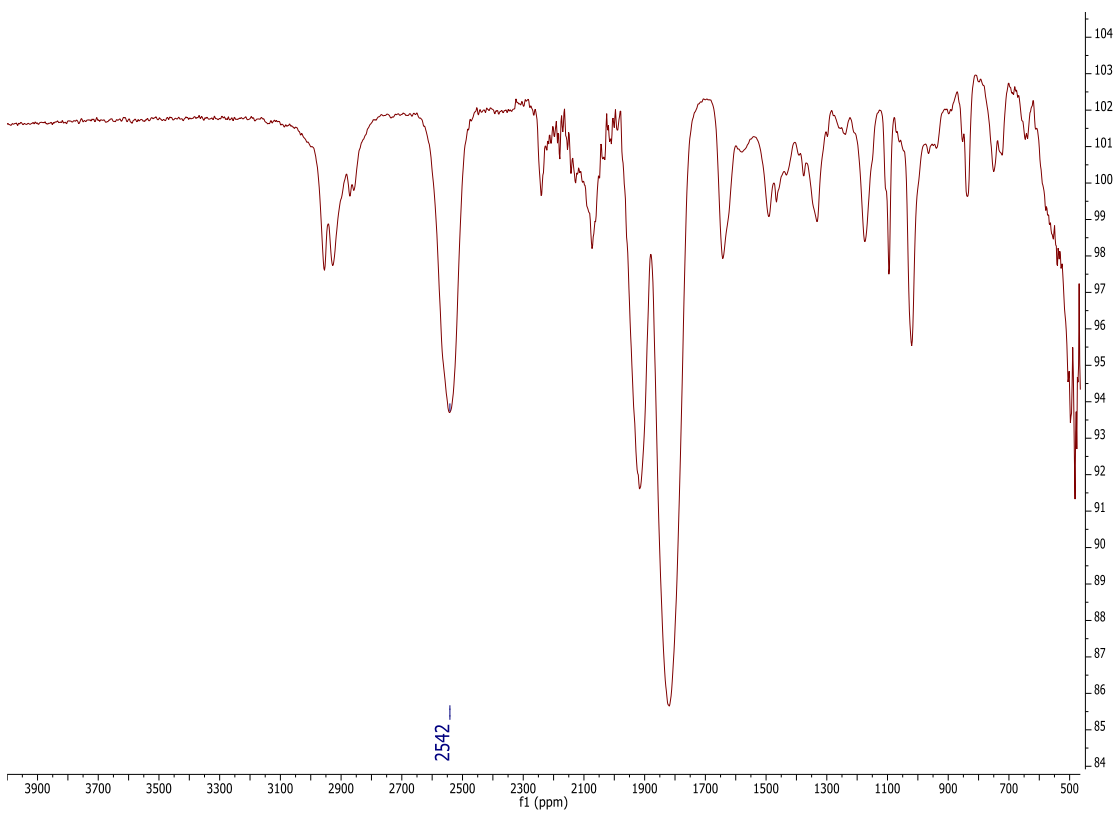


Fig. S38. IR spectrum of solid $\text{Li}_2[10]$. The boron hydrides appear at 2542 & 2567 cm^{-1} .

X-Ray Structure Determination

Monoanionic Lithium Carbene Li[9]:

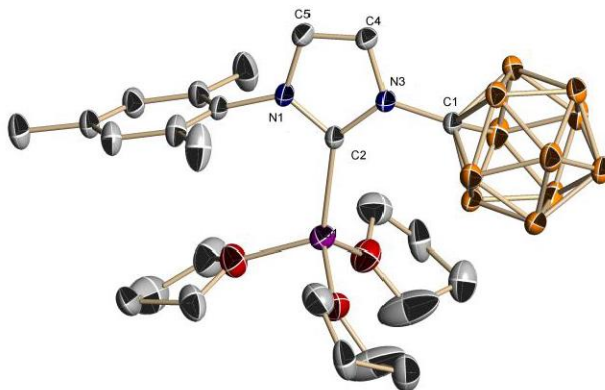


Fig. S39. Solid state structure of Li[9]. Hydrogen atoms are omitted for clarity.

A colorless prism fragment (0.532 x 0.455 x 0.379 mm³) was used for the single crystal x-ray diffraction study of C₃H₂N₂[CH₁₁B₁₁][C₉H₁₁Li][C₄H₈O]₃ (sample vL123MA_0m). The crystal was coated with paratone oil and mounted on to a cryo-loop glass fiber. X-ray intensity data were collected at 163(2) K on a Bruker APEX2 platform-CCD x-ray diffractometer system (fine focus Mo-radiation, $\lambda = 0.71073 \text{ \AA}$, 50KV/30mA power). The CCD detector was placed at a distance of 5.0600 cm from the crystal.

A total of 4800 frames were collected for a sphere of reflections (with scan width of 0.3° in ω and ϕ , starting ω and 2θ angles of -30° , and ϕ angles of 0° , 90° , 120° , 180° , 240° , and 270° for every 600 frames, and 1200 frames with ϕ -scan from 0-360°, 10 sec/frame exposure time). The frames were integrated using the Bruker SAINT software package and using a narrow-frame integration algorithm. Based on a monoclinic crystal system, the integrated frames yielded a total of 90725 reflections at a maximum 2θ angle of 61.014° (0.70 \AA resolution), of which 5070 were independent reflections ($R_{\text{int}} = 0.0355$, $R_{\text{sig}} = 0.0124$, redundancy = 17.9, completeness = 100%) and 3960 (78.1%) reflections were greater than $2\sigma(I)$. The unit cell parameters were, $\mathbf{a} = 15.1947(4) \text{ \AA}$, $\mathbf{b} = 12.6157(3) \text{ \AA}$, $\mathbf{c} = 16.6660(4) \text{ \AA}$, $\alpha = \beta = \gamma = 90^\circ$, $V = 3194.74(14) \text{ \AA}^3$, $Z = 4$, calculated density $D_c =$

1.145 g/cm³. Absorption corrections were applied (absorption coefficient $\mu = 0.066 \text{ mm}^{-1}$; min/max transmission = 0.966/0.975) to the raw intensity data using the SADABS program.

The Bruker SHELXTL software package was used for phase determination and structure refinement. The distribution of intensities ($E^2-1 = 0.997$) and systematic absent reflections indicated two possible space groups, Pna2(1) and Pnma. The space group Pnma (#62) was later determined to be correct. Direct methods of phase determination followed by two Fourier cycles of refinement led to an electron density map from which most of the non-hydrogen atoms were identified in the asymmetric unit of the unit cell. With subsequent isotropic refinement, all of the non-hydrogen atoms were identified. There was half a molecule of $\text{C}_3\text{H}_2\text{N}_2[\text{CH}_{11}\text{B}_{11}][\text{C}_9\text{H}_{11}]\text{Li}[\text{C}_4\text{H}_8\text{O}]_3$ present in the asymmetric unit of the unit cell. All three THF molecules were modeled with disorder (the THF disorder site occupancy ratios were 50%/50%, 56%/44%, and 56%/44%). The molecule was located at the mirror plane perpendicular to the **b**-axis.

Atomic coordinates, isotropic and anisotropic displacement parameters of all the non-hydrogen atoms were refined by means of a full matrix least-squares procedure on F^2 . The H-atoms were included in the refinement in calculated positions riding on the atoms to which they were attached. The refinement converged at $R1 = 0.0513$, $wR2 = 0.1426$, with intensity $I > 2\sigma(I)$. The largest peak/hole in the final difference map was 0.338/-0.186 e/Å³. CCDC #1028440 has the complete crystallographic information.

Table 1. Crystal data and structure refinement for vL123MA_0m.

Identification code	vL123MA_0m	
Empirical formula	C ₂₅ H ₄₈ B ₁₁ Li N ₂ O ₃	
Formula weight	550.50	
Temperature	163(2) K	
Wavelength	0.71073 Å	
Crystal system	Orthorhombic	
Space group	P n m a	
Unit cell dimensions	a = 15.1947(4) Å	$\alpha = 90^\circ$.
	b = 12.6157(3) Å	$\beta = 90^\circ$.
	c = 16.6660(4) Å	$\gamma = 90^\circ$.
Volume	3194.74(14) Å ³	
Z	4	
Density (calculated)	1.145 Mg/m ³	
Absorption coefficient	0.066 mm ⁻¹	
F(000)	1176	
Crystal size	0.532 x 0.455 x 0.379 mm ³	
Theta range for data collection	1.814 to 30.507°.	
Index ranges	-21 ≤ h ≤ 21, -18 ≤ k ≤ 18, -23 ≤ l ≤ 23	
Reflections collected	90725	
Independent reflections	5070 [R(int) = 0.0355]	
Completeness to theta = 25.242°	100.0 %	
Absorption correction	Semi-empirical from equivalents	
Refinement method	Full-matrix least-squares on F ²	
Data / restraints / parameters	5070 / 20 / 261	
Goodness-of-fit on F ²	1.037	
Final R indices [I > 2σ(I)]	R1 = 0.0513, wR2 = 0.1426	
R indices (all data)	R1 = 0.0667, wR2 = 0.1565	
Extinction coefficient	n/a	
Largest diff. peak and hole	0.338 and -0.186 e.Å ⁻³	

Dianionic Lithium Carbene Li₂[10]:

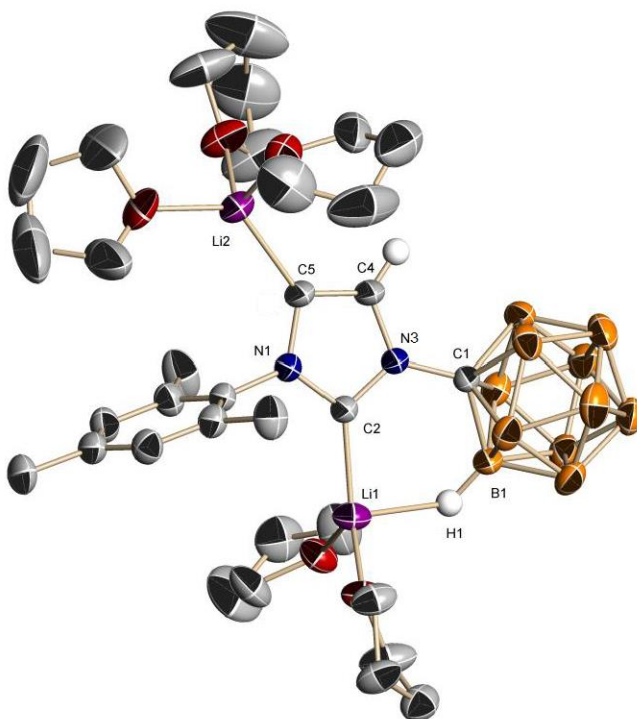


Fig. S40. Solid state structure of **Li₂[10]**. Hydrogen atoms (except C5-H and H1) are omitted for clarity.

A colorless prism fragment (0.518 x 0.428 x 0.261 mm³) was used for the single crystal x-ray diffraction study of C₃HN₂[CH₁₁B₁₁][C₉H₁₁Li₂[C₄H₈O]₅·[C₄H₈O]_{0.48} (sample vL131SF_0m). The crystal was coated with paratone oil and mounted on to a cryo-loop glass fiber. X-ray intensity data were collected at 200(2) K on a Bruker APEX2 platform-CCD x-ray diffractometer system (fine focus Mo-radiation, $\lambda = 0.71073 \text{ \AA}$, 50KV/30mA power). The CCD detector was placed at a distance of 5.0600 cm from the crystal.

A total of 3600 frames were collected for a sphere of reflections (with scan width of 0.3° in ω , starting ω and 2θ angles of -30° , and ϕ angles of 0° , 90° , 120° , 180° , 240° , and 270° for every 600 frames, 60 sec/frame exposure time). The frames were integrated using the Bruker SAINT software package and using a narrow-frame integration algorithm. Based on a orthorhombic crystal system, the integrated frames yielded a total of 102718 reflections at a maximum 2θ angle of 60.064° (0.71 \AA resolution), of which 13139 were

independent reflections ($R_{\text{int}} = 0.0286$, $R_{\text{sig}} = 0.0155$, redundancy = 7.8, completeness = 99.9%) and 11345 (86.3%) reflections were greater than $2\sigma(I)$. The unit cell parameters were, $\mathbf{a} = 15.9089(11) \text{ \AA}$, $\mathbf{b} = 26.7369(19) \text{ \AA}$, $\mathbf{c} = 10.5610(8) \text{ \AA}$, $\alpha = \beta = \gamma = 90^\circ$, $V = 4492.2(6) \text{ \AA}^3$, $Z = 4$, calculated density $D_c = 1.087 \text{ g/cm}^3$. Absorption corrections were applied (absorption coefficient $\mu = 0.066 \text{ mm}^{-1}$; min/max transmission = 0.967/0.983) to the raw intensity data using the SADABS program.

The Bruker SHELXTL software package was used for phase determination and structure refinement. The distribution of intensities ($E^2 - 1 = 0.766$) and systematic absent reflections indicated two possible space groups, Pnnm and Pnn2. The space group Pnn2 (#34) was later determined to be correct. Direct methods of phase determination followed by two Fourier cycles of refinement led to an electron density map from which most of the non-hydrogen atoms were identified in the asymmetric unit of the unit cell. With subsequent isotropic refinement, all of the non-hydrogen atoms were identified. There was one molecule of $\text{C}_3\text{HN}_2[\text{CH}_{11}\text{B}_{11}][\text{C}_9\text{H}_{11}]\text{Li}_2[\text{C}_4\text{H}_8\text{O}]_5$ and one partially occupied [48%] $\text{C}_4\text{H}_8\text{O}$ solvent molecule present in the asymmetric unit of the unit cell. Three of the five THF molecules bonded to the two Li-atoms were modeled with disorder (the THF disorder site occupancy ratios were 50%/50%, 56%/44%, and 56%/44%). The partially occupied THF solvent molecule was located at the 2-fold rotation axis parallel to the \mathbf{c} -axis. Note that the crystal shattered at about 135K.

Atomic coordinates, isotropic and anisotropic displacement parameters of all the non-hydrogen atoms were refined by means of a full matrix least-squares procedure on F^2 . The H-atoms were included in the refinement in calculated positions riding on the atoms to which they were attached. The refinement converged at $R1 = 0.0551$, $wR2 = 0.1520$, with intensity $I > 2\sigma(I)$. The largest peak/hole in the final difference map was 0.400/-0.252 e/\AA^3 . CCDC #1028443 has the complete crystallographic information.

Table 2. Crystal data and structure refinement for vL131SF_0m.

Identification code	vL131SF_0m
Empirical formula	C _{34.93} H _{66.85} B ₁₁ Li ₂ N ₂ O _{5.48}
Formula weight	735.40
Temperature	200(2) K
Wavelength	0.71073 Å
Crystal system	Orthorhombic
Space group	P n n 2
Unit cell dimensions	a = 15.9089(11) Å α = 90°. b = 26.7369(19) Å β = 90°. c = 10.5610(8) Å γ = 90°.
Volume	4492.2(6) Å ³
Z	4
Density (calculated)	1.087 Mg/m ³
Absorption coefficient	0.066 mm ⁻¹
F(000)	1581
Crystal size	0.518 x 0.428 x 0.261 mm ³
Theta range for data collection	1.489 to 30.032°.
Index ranges	-22 ≤ h ≤ 22, -37 ≤ k ≤ 37, -14 ≤ l ≤ 14
Reflections collected	102718
Independent reflections	13139 [R(int) = 0.0286]
Completeness to theta = 25.242°	99.9 %
Absorption correction	Semi-empirical from equivalents
Refinement method	Full-matrix least-squares on F ²
Data / restraints / parameters	13139 / 1296 / 804
Goodness-of-fit on F ²	1.054
Final R indices [I > 2σ(I)]	R1 = 0.0551, wR2 = 0.1520
R indices (all data)	R1 = 0.0637, wR2 = 0.1624
Absolute structure parameter	-0.03(11)
Extinction coefficient	n/a
Largest diff. peak and hole	0.400 and -0.252 e.Å ⁻³

References:

1. T. Jelinek, J. Plesek, S. Hermanek, B. Stibr, *Collect. Czech. Chem. Commun.*, 1986, **51**, 819.
2. A. Furstner, M. Alcarazo, V. Cesar, C. W. Lehmann, *Chem. Comm.*, 2006, 2176.